FEBS Letters 580 (2006) 3706–3714

Intravenous administration of mannosylated cationic liposome/NFκB decoy complexes effectively prevent LPS-induced cytokine production in a murine liver failure model

Yuriko Higuchi, Shigeru Kawakami, Machiko Oka, Yoshiyuki Yabe, Fumiyoshi Yamashita, Mitsuru Hashida*

Department of Drug Delivery Research, Graduate School of Pharmaceutical Sciences, Kyoto University, 46-29 Yoshidashimoadachi-cho, Sakyo-ku, Kyoto 606-8501, Japan

Received 16 May 2006; accepted 25 May 2006

Available online 6 June 2006

Edited by Laszlo Nagy

Abstract **The purpose of this study was to inhibit endotoxin induced cytokines production and liver injury by liver non-parenchymal cell (NPC) selective delivery of nuclear factor κB (NFκB) decoy using mannosylated cationic liposomes (Man-liposomes). In this study, we examined the distribution, inhibitory effect on cytokines production and ALT/AST of intravenously injected Man-liposome/NFκB decoy complex. Man-liposome/[^{32}P] NFκB decoy complexes mostly accumulated in the liver, preferentially in NPC. In a murine lipopolysaccharide-induced liver failure model, the production of tumor necrosis factor-α (TNFα), IFNγ, IL1-β, ALT and AST were effectively reduced by Man-liposome complexes. However, cationic or galactosylated cationic liposome complexes could not inhibit TNFα production.**

Keywords: Mannosylated cationic liposome; Mannose receptor; NFκB decoy; Macrophage; Tumor necrosis factor-α

1. Introduction

Endotoxin syndrome is a particularly grave complication because bacteriologically proven infection occurs in up to 80% of patients with hepatic failure [1]. It is known that endotoxin syndrome, caused by infection of gram-negative bacteria, is a systemic inflammatory response mediated by several cytokines including tumor necrosis factor-α (TNFα), IL-1β, IFNγ, IL-12, etc., through nuclear factor κB (NFκB) activation in vivo [2]. Furthermore, increasing evidence indicates that Kupffer cells, hepatic resident macrophages, play a pivotal role in the production of the inflammatory cytokine response under a variety of stress conditions, such as hepatic failure, including viral infection [3,4]. Therefore, the prevention of cytokine overproduction by Kupffer cells would be an important factor for the treatment of endotoxin syndrome.

*Corresponding author. Fax: +81 75 753 4575.
E-mail address: hashidam@pharm.kyoto-u.ac.jp (M. Hashida).

Abbreviations: TNFα, tumor necrosis factor-α; LPS, lipopolysaccharide; NFκB, nuclear factor κB; PC, parenchymal cell; NPC, non-parenchymal cell

Several reports have demonstrated that NFκB activation in macrophages causes inflammatory cytokines and adhesion molecule production in a wide variety of types of inflammation and disease [5,6]. Recently Wrighton et al. [7] and Foxwell et al. [8] reported that adenoviral gene transfer of super-repressor IκB produced effective suppression of NFκB, however, the inflammatory reaction and high immunogenesity of the adenoviral vector itself posed a serious obstacle to in vivo therapy. In contrast, the decoy strategy has been developed and considered a useful tool as a new class of anti-gene strategy. In this NFκB decoy, double stranded oligonucleotides containing NFκB binding sequences, bind to activated-NFκB consequently inhibiting transcription by NFκB [9–11]. Therefore, the NFκB decoy approach enables us to treat diseases by suppression of target gene expression without high immunogenisity [12].

To establish NFκB decoy therapy, it is necessary to develop a Kupffer cell-targeting carrier for NFκB decoy to treat liver disease because of the low accumulation in Kupffer cells after intravenous injection of NFκB decoy [13]. As far as the liver-specific delivery of NFκB decoy is concerned, Ogushi et al. [14] recently demonstrated that NFκB decoy, transferred by fusigenic liposomes with hemagglutinating virus of Japan (HVJ liposomes) from the portal vein, effectively suppressed endotoxin-induced fatal liver injury in mice. However, intraportal injection is difficult in clinical situations because it needs a skilful surgical technique and increases the burden on the patient. Although intravenous injection is the most simple method, HVJ liposomes cannot accumulate in the liver following intravenous injection, because HVJ liposomes fuse to cells in a non-specific manner [15,16]. As a consequence, oligonucleotide is non-specifically delivered by HVJ liposomes to the lung, spleen and kidneys after intravenous injection [16]. In fact, Ogushi et al. achieved a therapeutic effect only by intraportal injection of HVJ liposomes not by intravenous injection. Moreover, because Kupffer cells account for only 15% of the total liver cells [17], non-specific fusion with HVJ liposomes would cause an increase in the NFκB decoy dose. Furthermore, preparing HVJ liposomes is complicated with irradiation to remove viral toxicity and centrifugation to remove free HVJ, etc. [18]. Therefore, a Kupffer cell-targeting carrier for NFκB decoy would lead to a more effective treatment for lipopolysaccharide (LPS) induced liver injury.

To develop a Kupffer cell-specific targeting carrier for NFκB decoy, receptor-mediated uptake is a promising

0014-5793/$32.00 © 2006 Published by Elsevier B.V. on behalf of the Federation of European Biochemical Societies.
doi:10.1016/j.febslet.2006.05.059

approach [19] because Kupffer cells are known to express large numbers of mannose receptors on their surface [17]. Recently we designed cholesten-5-yloxy-*N*-{4-[(1-imino-2-D-thiomannosyl-ethyl)-amino]butyl} formamide (Man-C4-Chol) to prepare mannosylated cationic liposomes (Man-liposomes) for mannose receptor-mediated plasmid DNA (pDNA) delivery [20–23]. Man-C4-Chol can be stably incorporated into liposomes and easily recognized by mannose receptors under in vivo conditions [24]. Furthermore, because Man-C4-Chol has an amino group for binding to pDNA via electrostatic interaction and a mannose residue for recognition by mannose receptors, a high density of mannose residues can be provided on the surface of liposome without affecting the binding ability of the cationic liposomes to pDNA [20]. Furthermore, we demonstrated that the highest gene expression observed for pDNA complexed with Man-liposomes via mannose receptor-mediated endocytosis [25].

Since NFκB decoy has anionic charges on its surface, we believe that NFκB decoy could form a complex with cationic liposome mediated by electrostatic interaction. In addition, since the size of NFκB decoy (20 base pairs) was more than 300-times smaller than pDNA (about 7000 base pairs), a large amount of NFκB decoy could form a complex with Man-liposomes. In this respect, a smaller amount of Man-liposomes could effectively deliver NFκB decoy compared with pDNA delivery. The reduction in the dose of carrier would be attractive for clinical therapy because of the reduced side-effects and low cost. The purpose of this study was to establish decoy therapy for endotoxin-induced liver disease. We developed a potential carrier for Kupffer cell targeting delivery of NFκB decoy after intravenous injection, demonstrating the first in vivo therapy by targeted delivery of NFκB decoy via intravenous injection. Results were compared with naked NFκB decoy and its complex with bare cationic liposomes.

2. Materials and methods

2.1. Materials

N-(4-aminoethyl) carbamic acid *tert*-butyl ester and *N*-[1-(2,3-dioleyloxy)propyl]-*n*,*n*,*n*-tri-methylammonium chloride (DOTMA) were purchased from Tokyo Kasei Kogyo Co. Ltd. (Tokyo, Japan). Dioleoylphosphatidylethanolamine (DOPE) was purchased from Avanti Polar Lipids Inc. (Alabaster, AL, USA). Cholesteryl chloroformate, heparin LPSs (from salmonella enterica serotype Minnesota Re 595) and collagenase were purchased from Sigma Chemicals Pty. Ltd. (St. Louis, MO, USA). Oligonucleotides (NFκB decoy: 5′-AGTTGAGGGGACTTTCCCAGGC-3′, 5′-GCCTGGGAAAGTCCCCTCAACT-3′; random decoy: 5′-TTGCCGTACCTGACTTAGCC-3′, 5′-GGCTAAGTCAGGTACGGCAA-3′) were purchased from Operon Biotechnologies Inc. (Tokyo, Japan). Ethylene glycol-bis(β-aminoethylether)-*N*,*N*,*N*′,*N*′-tetraacetic acid (EGTA), Clear-Sol I and cholesterol were purchased from Nacalai Tesque Inc. (Kyoto, Japan). MEGALABEL™ 5′-End Labeling Kit was purchased from Takara Bio Inc. (Shiga, Japan). Soluene-350 was purchased from Perkin–Elmer Inc. (Boston, MA, USA). NAP-5 column was purchased from Amersham Biosciences Co. (Piscatway, NJ, USA). Trypan blue was purchased from Invitrogen Co. (Grand Island, NY, USA). Mouse TNFα BD OptEIA™ ELISA Kit was purchased from Becton, Dickinson and Company (Mississauga, Canada). Fraction-PREP™ Nuclear/Cytosol Fraction Kit was purchased from BioVision Inc. (Mountain View, CA, USA). Transaminase C II test wako was purchased from Wako Pure Chemical Industries Ltd. (Osaka, Japan). Chemiluminescent NFκB Activation Assay Kit was purchased from Oxford Biomedical Research Inc. (Oxford, MI, USA).

2.2. Animals

Female ICR mice (5-week old, 22–24 g) or female C57BL/6 mice (6-week old, 18–20 g) were obtained from Shizuoka Agricultural Cooperative Association for Laboratory Animals (Shizuoka, Japan). All animal experiments were carried out in accordance with the Principles of Laboratory Animal Care as adopted and promulgated by the US National Institutes of Health and with the Guidelines for Animal Experiments of Kyoto University.

2.3. Radiophosphorylation of decoy oligonucleotides

Annealed NFκB decoy were labeled with [γ-^{32}P] ATP using MEGALABELTM 5′-End Labeling Kit with some modification as reported previously [13]. Briefly, oligonucleotides, [γ-^{32}P] ATP and T4 polynucleotide kinase were mixed in phosphorylation buffer. After 30 min incubation at 37 °C, the mixture was incubated for 10 min at 70 °C in order to inactivate T4 polynucleotide kinase. Then, the mixture was purified by gel chromatography using a NAP 5 column and eluted with 10 mM Tris–Cl and 1 mM EDTA (pH 8.0). The fractions containing derivatives were selected based on their radioactivity.

2.4. Synthesis of Man-C4-Chol

Man-C4-Chol was synthesized as reported previously [20]. Briefly, cholesteryl chloroformate and *N*-(4-aminobutyl)carbamic acid *tert*-butyl ester were reacted in chloroform for 24 h at room temperature. A solution of trifluoroacetic acid and chloroform was added dropwise and the mixture was stirred for 4 h at 4 °C. The solvent was evaporated to obtain *N*-(4-aminobutyl)-(cholesten-5-yloxyl)formamide which was then combined with 2-imino-2-methoxyethyl-1-thiomannoside and the mixture was stirred for 24 h at room temperature. After evaporation, the resultant material was suspended in water, dialyzed against distilled water for 48 h (12 kDa cut-off dialysis tubing), and then lyophilized. Gal-C4-Chol was also synthesized by the same method using galactose instead of mannose.

2.5. Preparation of liposomes and their complex with NFκB decoy

Man-liposomes, Gal-liposomes or DOTMA/cholesterol liposomes were prepared as reported previously [20]. Briefly, Man-C4-Chol, Gal-C4-Chol or DOTMA was mixed with DOPE or cholesterol, respectively, in chloroform at a molar ratio of and the mixture was dried, vacuum desiccated, and resuspended in sterile 5% dextrose. After hydration, the dispersion was sonicated for 10 min in a bath sonicator and then for 3 min in a tip sonicator to form liposomes.

The preparation of liposome/NFκB decoy complexes for in vivo use was carried out by the method of Kawakami et al. [25]. Equal volumes of NFκB decoy and stock liposome solution were diluted with 5% dextrose at room temperature. Then, the NFκB decoy solution was added rapidly to the liposome solution and the mixture was agitated rapidly by pumping it up and down twice in the pipet tip. The mixture was then left at room temperature for 30 min. The theoretical charge ratio of lipid/NFκB decoy was calculated as a molar ratio of Man-C4-Chol (monovalent) to a nucleotide unit (average molecular weight 330) [21,26,27].

The particle size of the liposomes and liposomes/NFκB decoy complexes were measured using dynamic light scattering spectrophotometer (LS-900, Otsuka Electronics, Osaka, Japan). The zeta potential of liposomes and liposome/NFκB decoy complexes were measured by Nano ZS (Malvern Instruments Ltd., Malvern, WR, UK).

2.6. In vivo distribution

In vivo distribution was examined as previously reported [13]. NFκB decoy complexed with liposomes in 300 μl 5% dextrose solution was intravenously injected into mice. Blood was collected from the vena cava at 1, 5, 10, 30, 60 min, and mice were killed at each collection time point. Liver, kidney, spleen, heart and lung were removed, washed with saline, blotted dry, and weighed. Immediately prior to blood collection, urine was also collected directly from the urinary bladder. 10 μl of blood and 200 μl of urine, and a small amount of each tissue were digested with Soluene-350 (0.7 μl for blood, urine and tissues) by incubation overnight at 54 °C. Following digestion, 0.2 ml isopropanol, 0.2 ml 30% hydroxyperoxide, 0.1 ml 5 M HCl, and 5.0 ml Clear-Sol I were added. The samples were stored overnight, and radioactivity was measured in a scintillation counter (LSA-500, Beckman, Tokyo, Japan).

2.7. Intrahepatic distribution

Intrahepatic distribution of [^{32}P] NFκB decoy complexed with Man-liposomes was determined as in our previous report [24]. Five minutes after intravenous injection of NFκB decoy, Man-liposome/NFκB decoy or cationic liposome/NFκB decoy complex, each mouse was anesthetized with diethyl ether and the liver was perfused with preperfusion buffer (Ca^{2+}, Mg^{2+}-free Hanks buffer, pH 7.4, containing 1000 U/L heparin and 0.19 g/L EGTA) for 6 min at 5 ml/min followed by Hanks buffer containing 5 mM $CaCl_2$ and 220 U/ml collagenase (Type I) (pH 7.4) for 6 min at 5 ml/min. After discontinuation of the perfusion, liver was excised and liver cells were dispersed in ice-cold Hanks-HEPES buffer. The cell suspension was filtered through cotton gauze, followed by centrifugation at 50 × *g* for 1 min at 4 °C. The pellet containing parenchymal cells (PC) was washed 4 times with ice-cold Hanks-HEPES buffer. The supernatant containing non-parenchymal cell (NPC) was collected and purified by centrifugation at 50 × *g* for 1 min at 4 °C (4 times). PC and NPC suspensions were centrifuged at 340 × *g* for 10 min. PC and NPC were then resuspended separately in ice-cold Hanks-HEPES buffer (final volume 2 ml). The cell number and viability were determined by the trypan blue exclusion method. The radioactivity of 500 μl of each cell suspension was measured by the same method as for the in vivo distribution.

2.8. Animal treatment protocol

For cytokine secretion assessment, blood was collected from ICR mice 1 h after intravenous injection of LPS (0.4 mg/kg). The blood was allowed to coagulate for 2–3 h at 0.4 °C and serum was isolated as the supernatant fraction following centrifugation at 2000 × *g* for 20 min. The serum samples were immediately stored at −80 °C. The amounts of TNFα, IL-1β and IFN-γ were analyzed using an Opti-EIA™ ELISA Kit according to the manufacturer's protocol. For severe liver injury model, C57BL/6 mice were injected intraperitoneally with LPS (0.05 mg/kg) and D-galactosamine (1000 mg/kg) in pyrogen-free saline. The blood was allowed to coagulate for 2–3 h at 4 °C and serum was isolated as the supernatant fraction following centrifugation at 2000 × *g* for 20 min. Serum ALT and AST were measured with transaminase C II test wako according to the manufacturer's protocol.

2.9. Enzyme immunoassay for determination of the amount of nuclear NFκB

Liver was removed, washed with ice-cold saline, and blotted dry. A small amount of liver was homogenized in phosphate-buffered saline. Pellets of cells were obtained by centrifugation at 500 × *g* for 2 min, and a nuclear extract was prepared using a Nuclear/Cytosol Fraction Kit. The amounts of NFκB in the nuclei were measured with an NFκB Activation Assay Kit according to the manufacturer's protocol.

2.10. Statistical analysis

Statistical comparisons were performed by Student's *t* test for two groups and one-way ANOVA for multiple groups. Post hoc multiple comparisons were made by using Turkey's test.

3. Results

3.1. Particle size and zeta potential of Man-liposomes and their complex with NFκB decoy

Table 1 summarizes the mean diameter and zeta potential of liposomes or liposome/NFκB decoy complex in 5% dextrose. The mean diameter of the Man-liposome/NFκB decoy complex was less than 100 nm. After forming a complex with NFκB decoy, the charge on the surface of Man-liposome/NFκB decoy complex slightly decreased and the mean diameter was not changed.

Table 1
The mean particle sizes and zeta potential of liposome and liposome/NFκB decoy complexes

	Particle size (nm)	Zeta potential (mV)
Man-liposome	64.6 ± 1.70	61.4 ± 0.91
Man-liposome complex	61.6 ± 1.58	54.7 ± 0.60

3.2. Man-liposome/NFκB decoy complex rapidly and highly accumulated in liver after intravenous injection

Fig. 1 shows the time-courses of the radioactivity in blood, kidney, spleen, liver, lung, muscle and heart after intravenous injection of naked [^{32}P] NFκB decoy or [^{32}P] NFκB decoy complexed with Man-liposomes or cationic liposomes. Ten minutes after the intravenous injection of Man-liposome/[^{32}P] NFκB decoy complex, about 80% of the dose accumulated in the liver. However, naked [^{32}P] NFκB decoy was rapidly excreted in the urine and gradually accumulated in the kidney. Also, cationic liposome/[^{32}P] NFκB decoy complex gradually accumulated in the liver after rapid accumulation in the lung.

3.3. Man-liposome/NFκB decoy complex preferentially taken up by NPC

After intravenous injection of Man-liposome/[^{32}P] NFκB decoy complex, the radioactivity in the liver was preferentially recovered from the NPC fraction with the radioactivity ratio of NPC to PC (NPC/PC ratio on a cell-number basis) in the liver being approximately 2.6 (Fig. 2). In contrast, naked [^{32}P] NFκB decoy had an NPC/PC ratio of 0.66 (Fig. 2) and the cationic liposome/[^{32}P] NFκB decoy complex had NPC/PC ratio of 0.75 (Fig. 2). The total liver accumulation of Man-liposome/[^{32}P] NFκB decoy complex was higher than that of naked [^{32}P] NFκB decoy.

3.4. Man-liposome/NFκB decoy complex effectively suppressed inflammatory cytokine production

The serum concentration of TNFα was assessed using ELISA to confirm that NFκB decoy complexed with Man-liposomes effectively suppressed the production of inflammatory cytokines induced by LPS in vivo (Fig. 3). After intravenous injection of LPS, the highest serum concentration of TNFα was observed at 1 h (data not shown). Control mice were only treated with LPS for 1 h. A dose-dependence in the suppression effect of Man-liposome/NFκB decoy complex was observed (Fig. 3A).

Thirty micrograms of NFκB decoy complexed with Man-liposomes markedly inhibited the production of TNFα in serum compared LPS alone. However, the same amount of NFκB decoy complexed with cationic liposomes or Gal-liposomes could not inhibit TNFα production (Fig. 3B). Moreover, 30 μg of a random decoy of almost the same size but with no NFκB binding sequence had no inhibitory effect on TNFα production (Fig. 3C). These results indicated that the inhibitory effect of TNFα production depended on the sequence of the NFκB decoy.

The serum concentrations of IL-1β and IFNγ were also assayed by ELISA (Fig. 4). The serum level of IL-1β and IFNγ induced by LPS was significantly suppressed by intravenous administration of Man-liposome/NFκB decoy complex (Fig. 4A and B). IFNγ is partly produced in response to LPS-induced inflammatory cytokines (TNFα, IL-12, etc.). Therefore, the inhibition of IFNγ by Man-liposome/NFκB decoy complex indicated secondary inhibition following to the inhibition of the upstream cytokines.

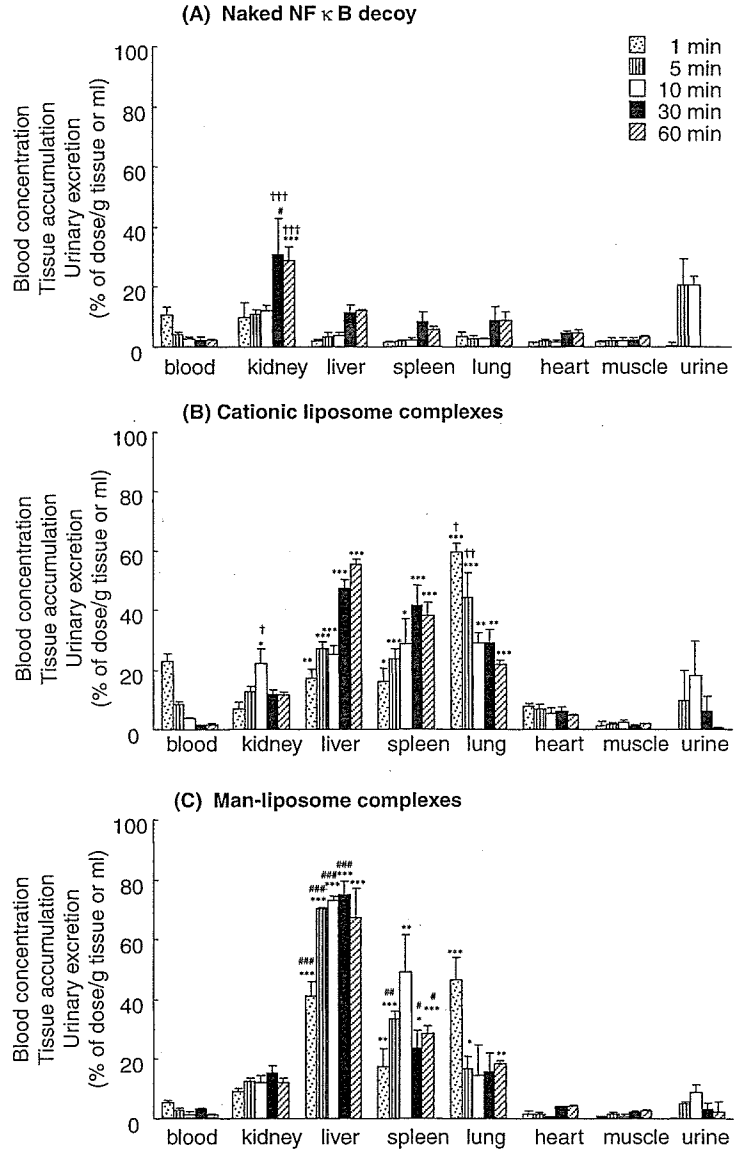

Fig. 1. Blood concentration, tissue accumulation and urinary excretion of ^{32}P-labeled naked NFκB decoy (A), cationic liposome/^{32}P-labeled NFκB decoy complex (B) and Man-liposome/^{32}P-labeled NFκB decoy complex (C) after intravenous injection into mice. ^{32}P-labeled NFκB decoy was complexed with mannosylated liposomes or cationic liposomes at a charge ratio of 2.3:1.0 (+:−). Radioactivity was determined in blood, liver, lung, spleen, kidney, heart, muscle and urine after 1, 5, 10, 30 and 60 min. Each value represents the mean ± S.D. ($n = 3$). Significant difference: $^{***}P < 0.001$, $^{**}P < 0.01$, $^{*}P < 0.05$ vs. (naked NFκB decoy); $^{\#\#\#}P < 0.001$, $^{\#\#}P < 0.01$, $^{\#}P < 0.05$ vs. (cationic liposome complexes); and $^{\dagger\dagger\dagger}P < 0.001$, $^{\dagger\dagger}P < 0.01$, $^{\dagger}P < 0.05$ vs. (Man-liposome complexes).

3.5. Man-liposome/NFκB decoy complex effectively prevents severe liver injury

ALT or AST measured in serum provide an index of hepatocyte integrity. Leakage of ALT and AST into the extracellular compartment and a subsequent rise in serum reflect hepatocytes damage. These enzymes are significantly elevated at liver damage caused by LPS induced inflammatory cytokines. Only LPS treatment with ICR mice did not caused significantly rise serum ALT and AST level (data not shown). Therefore, LPS and D-(+)-galactosamine treated C57BL/6 mice were used to determine therapeutic effect of Man-liposome/NFκB decoy complex for liver injury. The serum activity of ALT and AST increased after administration of LPS and D-(+)-galactosamine, which indicated severe liver injury. Although naked NFκB decoy did not prevent liver injury, Man-liposome/NFκB decoy complex significantly inhibit increase of ALT and AST level in the serum (Fig. 5). These results indicated Man-liposome/NFκB decoy complex could prevent LPS caused liver injury.

3.6. Man-liposome/NFκB decoy complex effectively prevents NFκB activation in nuclei

In response to inflammatory stimuli, IκB protein degraded and allowed NFκB to translocate into the nucleus to initiate gene expression of inflammatory cytokines. The amount of activated NFκB in the nuclei was measured by enzyme immu-

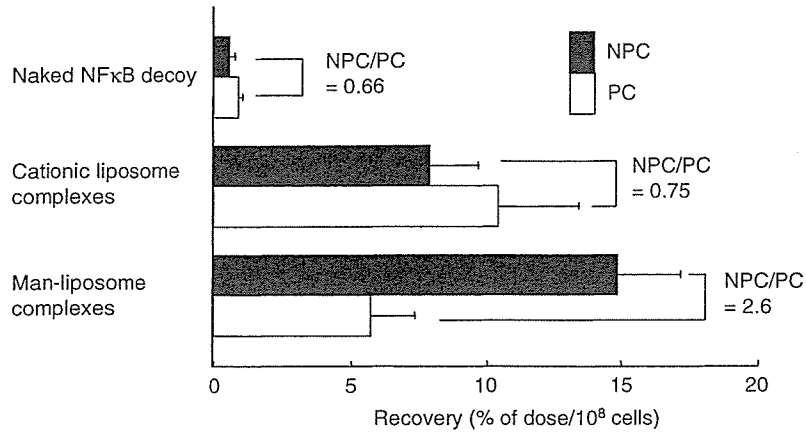

Fig. 2. Intrahepatic distribution of ^{32}P-labeled naked NFκB decoy, cationic liposome/^{32}P-labeled NFκB decoy complex and Man-liposome/^{32}P-labeled NFκB decoy complex after intravenous injection into mice. ^{32}P-labeled NFκB was complexed with mannosylated liposomes or cationic liposomes at a charge ratio of 2.3:1.0 (+:−). Radioactivity was determined in NPC (■) and PC (□). Each value represents the mean ± S.D. (n = 3).

noassay (EIA) to confirm directly the inhibitory effect of Man-liposome/NFκB decoy complex on the activation of NFκB. After LPS treatment, the amount of activated NFκB was dramatically increased. However, after injection of Man-liposome/NFκB decoy complex, the amount of activated NFκB in nuclei did not increase with LPS treatment (Fig. 6).

4. Discussion

Recently, new techniques to inhibit target gene expression using oligonucleotides, such as decoy oligonucleotides, antisense DNA, ribozyme and siRNA, have been developed, which are expected to be attractive treatments without side-effects on genome DNA compared with pDNA. However, oligonucleotides are easily degraded in blood and rapidly metabolized and, therefore, potential carriers have to be developed capable of carrying enough oligonucleotide to produce a therapeutic effect. As far as NFκB decoy therapy for endotoxin syndrome is concerned, since Kupffer cells play an important role of producing cytokines, NFκB decoy taken up by Kupffer cells could effectively inhibit NFκB-mediated inflammatory cytokine production. In this respect, in order to achieve a therapeutic effect with NFκB decoy, it is necessary to develop a Kupffer cell-targeting carrier for NFκB decoy. Previously, we have developed a novel pDNA carrier system for NPC targeting involving Man-liposomes, which could effectively achieve cell-specific transfer to NPC and macrophages in vivo and in vitro [20–22]. Man-liposomes are an attractive tool for NFκB decoy delivery to Kupffer cells, although the physicochemical properties, such as molecular weight and size, of the NFκB decoy and pDNA are very different. Therefore, the purpose of this study was to investigate the distribution and therapeutic effect of Man-liposome/NFκB decoy complex on endotoxin syndrome.

To investigate NPC selective delivery of NFκB decoy by Man-liposomes, the tissue and intrahepatic distribution of Man-liposome/[^{32}P] NFκB decoy complex were examined. In this study, Man-liposome/[^{32}P] NFκB decoy complex exhibited rapid and high accumulation in the liver (Fig. 1). This result was well concerned with the tissue accumulation of Man-liposome/pDNA complex after intravenous injection [22]. As far as intrahepatic distribution is concerned, the Man-liposome/NFκB decoy complex was preferentially taken up by NPC (Fig. 2). This result also agreed with the intrahepatic distribution of Man-liposome/pDNA complex [22]. Considering that mannose receptors are expressed on NPC [17], these results are in good agreement with the intrahepatic distribution of Man-liposome/NFκB decoy complex (Fig. 2). Moreover, Gal-liposome/NFκB decoy complex could not inhibit cytokine production, comparing to the same amount of NFκB decoy delivered by Man-liposome showed significantly inhibitory effect (Fig. 3B). Gal-liposome/NFκB decoy complex would be preferentially taken up by hepatocyte not by NPC, since a large number of asiaroglycoprotein receptor, which could recognize galactose, was expressed on hepatocyte not NPC [28]. These results supported the mannose receptor-mediated uptake of Man-liposome/NFκB decoy complex.

To determine the therapeutic effect of Man-liposome/NFκB decoy complex, we investigated the inhibitory effect on cytokine production and liver injury measuring serum ALT and AST. The inhibitory effect of Man-liposome/NFκB decoy complex on cytokine production was determined by measuring the serum concentration of LPS-induced TNFα, which induced other kinds of cytokine production and inflammation (Fig. 4). Man-liposome/NFκB decoy complex significantly inhibited the production of these cytokines compared with the same dose of naked NFκB decoy and bare cationic liposome/NFκB decoy. Increase of serum ALT and AST, which indicate hepatocytes injury caused by inflammatory cytokines, were also prevented by Man-liposome/NFκB decoy complex but not by naked NFκB decoy. These results suggest that NFκB decoy is effectively delivered to Kupffer cells by Man-liposomes. This result agrees with the intrahepatic distribution of Man-liposome/NFκB decoy complex after intravenous injection (Fig. 2).

In order to evaluate whether Man-liposome/NFκB decoy complex could inhibit NFκB-mediated transcription, the amount of activated NFκB in the nuclei was determined by EIA (Fig. 6). The amount of activated NFκB in the liver nuclei was reduced by Man-liposome/NFκB decoy complex, which

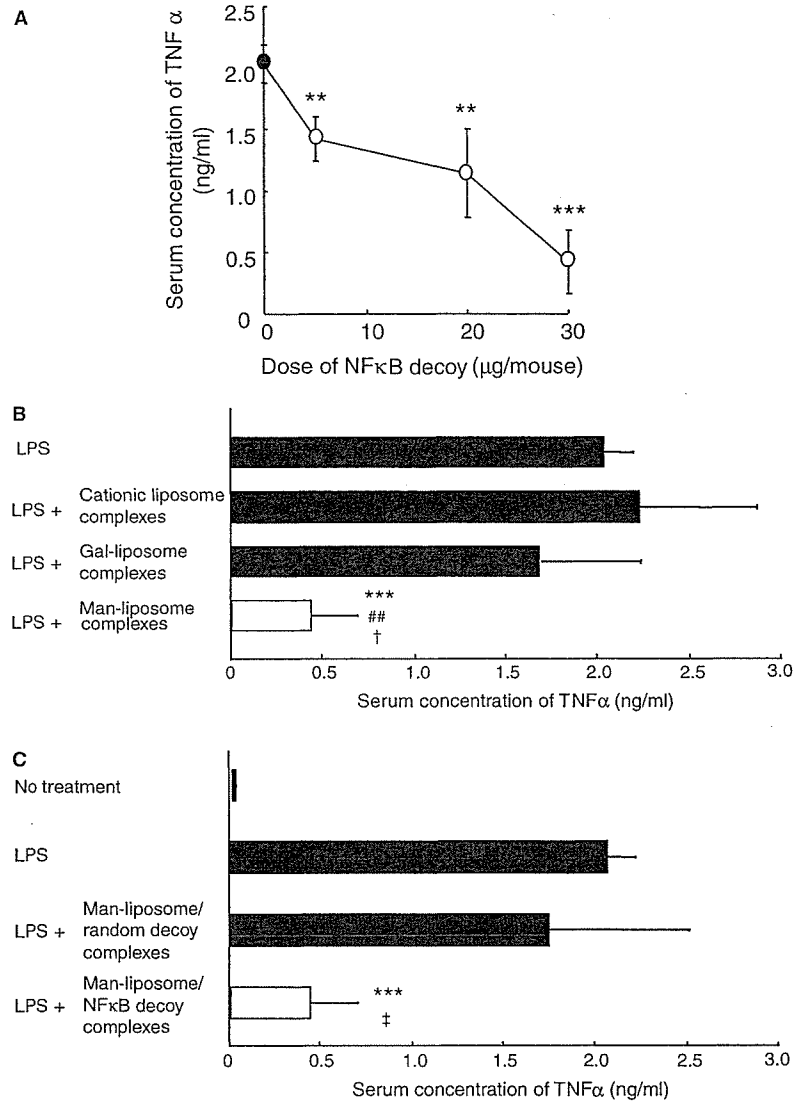

Fig. 3. Inhibitory effect of Man-liposome/NFκB decoy complex on the production of TNFα at different doses (A), several kinds of liposomes/NFκB decoy complexes (B) and the sequence of the decoy (C). Serum concentration of TNFα was determined by ELISA. One minute after intravenous administration of LPS, Man-liposome/NFκB decoy complex or Man-liposome/random decoy complex was intravenously injected into mice. Blood was collected from the vena cava at 1 h. Each value represents the mean ± S.D. ($n = 3, 4$). Significant difference: $^{***}P < 0.001$ vs. (LPS); $^{\#\#}P < 0.01$ vs. (LPS + cationic liposome complexes); $^{\dagger}P < 0.05$ vs. (LPS + Gal-liposome complexes); $^{\ddagger}P < 0.05$ vs. (LPS + Man-liposome/random decoy complex).

suggests that NFκB decoy binds to NFκB and inhibits translocation of NFκB into the nuclei. In addition, the production of IFNγ and IL-1β was also inhibited by the Man-liposome/NFκB decoy complex (Fig. 4), however, TNFα production could not be inhibited by the Man-liposome/random decoy complex. This result suggests that the sequence of the NFκB decoy is important for the inhibition of NFκB activation. These results confirm that NFκB decoy delivered by Man-liposomes is able to inhibit NFκB-mediated transcription. Since NFκB decoy can inhibit several kinds of NFκB-mediated cytokine production at the same time, cell-specific delivery of NFκB decoy will contribute to the novel therapy of other diseases involving several kinds of inflammatory cytokines.

As far as the therapy of liver disease evoked cytokine production by Kupffer cells is concerned, a Kupffer cell-targeting carrier is required for the effective therapy with NFκB decoy. To date, some carriers, including HVJ liposomes [14] and bare cationic liposomes [13], have been used as NFκB carriers to inhibit Kupffer cell cytokine production. However, because these carriers deliver NFκB decoy to any liver cells, the amount of NFκB decoy delivered to Kupffer cells is small considering that the number of Kupffer cells account for only 15% of the total number of liver cells [17]. In our previous study of bare cationic liposomes, after intravenous injection, bare cationic liposome/NFκB decoy complex gradually accumulated in the liver after rapid accumulation in the lung [13]. This rapid accumulation in the lung agreed with the distribution of cationic liposomes [29] and cationic liposome/pDNA complex [22,30]. As far as the intrahepatic distribution of bare cationic liposome/NFκB decoy is concerned, NPC/PC of cationic liposome/NFκB decoy was 1/3-fold lower than that of Man-liposome/NFκB decoy complex (Fig. 2). Considering

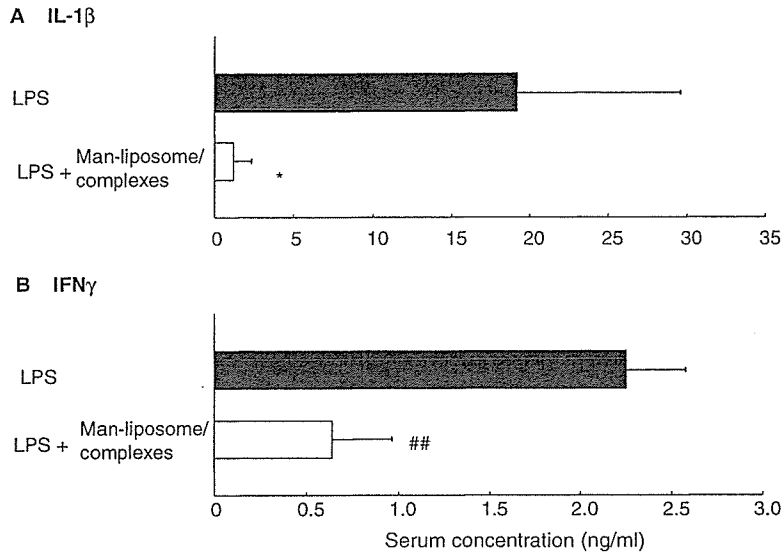

Fig. 4. Inhibitory effect of Man-liposome/NFκB decoy complex or Man-liposome/random decoy complex on the production of IL-1β (A) and IFNγ (B). One minute after intravenous administration of LPS, Man-liposome/NFκB decoy complex (30 μg/mouse) was intravenously injected into mice. Blood was collected from the vena cava at 3 h (IL-1β) and 6 h (IFNγ). Each value represents the mean ± S.D. ($n = 3$). Significant difference: $^{*}P < 0.05$ vs. (LPS in A); $^{\#\#}P < 0.01$ vs. (LPS in B).

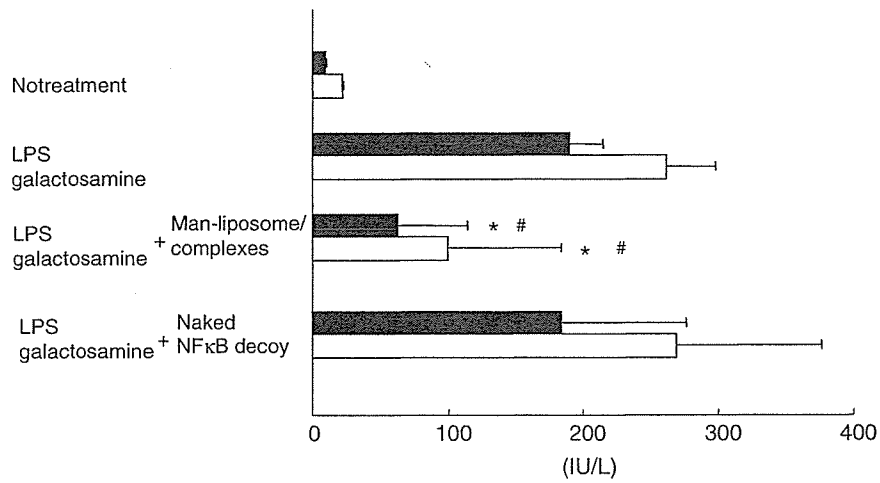

Fig. 5. Inhibitory effect of Man-liposome/NFκB decoy complexes on liver injury. One minute after intraperitoneal administration of LPS and D-(+)-galactosamine, Man-liposome/NFκB decoy complex (30 μg/mouse) or naked NFκB decoy were intravenously injected into mice. Blood was collected from the vena cava at 6 h. Serum concentration was determined in ALT (■) and AST (□). Each value represents the mean ± S.D. ($n \geqq 4$). Significant difference: $^{*}P < 0.05$ vs. (LPS); $^{\#}P < 0.05$ vs. (LPS + naked NFκB decoy).

the liver accumulation, these results suggested that the amount of NFκB decoy delivered by bare cationic liposomes is much lower than that by Man-liposomes. The results of this distribution study are in agreement with the pharmacological results showing that bare cationic liposome/NFκB decoy complex cannot suppress cytokine production while the same amount of NFκB decoy complexed with Man-liposomes significantly inhibits cytokine production (Fig. 3B). These results provide evidence that Kupffer cell-selective delivery is important for prevention of cytokines production.

In the present study, we demonstrated that Kupffer cell-selective delivery using Man-liposomes effectively inhibits cytokine production by Kupffer cells and liver injury caused by cytokines. Recently, we demonstrated that fucose-decorated bovine serum albumin, as a model macromolecular compound, was preferentially taken up by Kupffer cells via recognition by fucose receptors, which are uniquely expressed on Kupffer cells [31,32]. Therefore, fucose decoration of cationic liposomes may improve Kupffer cell-targeting delivery for NFκB decoy therapy. Based on the results of this study, we now intend to investigate fucosylated cationic liposomes.

In conclusion, Man-liposome/NFκB decoy complex showed specific accumulation in NPC and markedly suppressed the effect of NFκB-mediated inflammatory cytokine production and liver injury after intravenous injection. It was shown that NFκB decoy was delivered by Man-liposomes via mannose

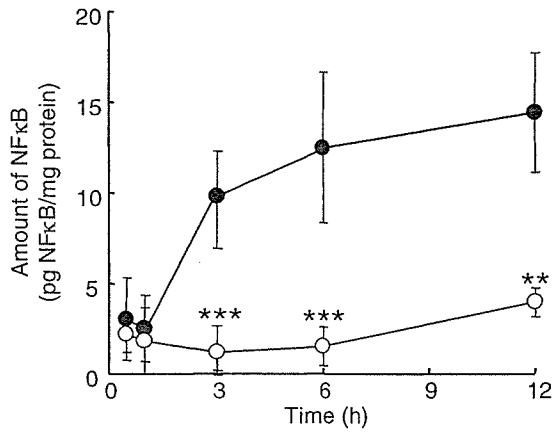

Fig. 6. Inhibitory effect of Man-liposome/NFκB decoy complex on NFκB activation in the nuclei. One minute after intravenous administration of LPS, Man-liposome/NFκB decoy complex (30 μg/mouse) (○) or 5% dextrose (●) was intravenously injected into mice. Liver was excised at 0.5, 1, 3, 6, 12 h and nuclear protein was extracted. Each value represents the mean ± S.D. ($n = 3$). Significant difference: $^{***}P < 0.001$, $^{**}P < 0.01$.

receptor recognition uptake. Following cell-specific delivery of NFκB decoy by Man-liposomes, NFκB in the nuclei in liver cells was attenuated and TNFα, IL1β and IFNγ production were inhibited at the same time. These observation lead us to believe that Man-liposomes are able to contribute to the development of new forms of therapy using oligonucleotides, such as antisense DNA, siRNA and so on.

Acknowledgements: This work was supported in part by Grant-in-Aids for Scientific Research from Ministry of Education, Culture, Sports, Science, and Technology of Japan, by Health and Labor Sciences Research Grants for Research on Advanced Medical Technology from the Ministry of Health, Labor and Welfare of Japan and by Radioisotope Research Center of Kyoto University.

References

[1] Roland, N., Wade, J., Davalos, M., Wendon, J., Philpott-Howars, J. and Williams, R. (2000) The system inflammatory response syndrome in acute liver failure. Hepatology 32, 734–739.
[2] Morrison, D.C. and Ryan, J.L. (1987) Endotoxins and disease mechanisms. Annu. Rev. Med. 38, 417–432.
[3] Iimuro, Y., Yamamoto, M., Kohno, H., Itakura, J., Fujii, H. and Matsumoto, Y. (1994) Blockade of liver macrophages by gadolinium chloride reduces lethality in endotoxemic rats analysis of mechanisms of lethality in endotoxemia. J. Leukoc. Biol. 55, 723–728.
[4] Arai, M., Mochida, S., Ohno, A., Ogata, I. and Fujiwara, K. (1993) Sinusoidal endothelial cell damage by activated macrophages in rat liver necrosis. Gastroenterology 104, 1466–1471.
[5] Pahl, H.L. (1999) Activations and target genes of Rel/NF-κB transcription factors. Oncogene 18, 6853–6866.
[6] Baeuerle, P.A. and Henkel, T. (1994) Function and activation of NF-κB in the immune system. Annu. Rev. Immunol. 12, 141–179.
[7] Wrighton, C.J., Hofer-Warbinek, R., Moll, T., Eytner, R., Bach, F.H. and de Martin, R. (1996) Inhibition of endothelial cell activation by adenovirus-mediated expression of IκBα, an inhibitor of the transcription factor NF-κB. J. Exp. Med. 183, 1013–1022.
[8] Foxwell, B., Browne, K., Bondeson, J., Clarke, C., de Martin, R., Brennan, F. and Feldmann, M. (1998) Efficient adenoviral infection with IκBα reveals that macrophage TNFα production in rheumatoid arthritis is NF-κB dependent. Proc. Natl. Acad. Sci. USA 95, 8211–8215.
[9] Bielinska, A., Shivdasani, R.A., Zhang, L.Q. and Nabel, G.J. (1990) Regulation of gene expression with double-stranded phosphorothioate oligonucleotides. Science 250, 997–1000.
[10] Morishita, R., Higaki, J., Tomita, N. and Ogihara, T. (1998) Application of transcription factor "decoy" strategy as means of gene therapy and study of gene expression in cardiovascular disease. Circ. Res. 82, 1023–1028.
[11] Morishita, R., Sugimoto, T., Aoki, M., Kida, I., Tomita, N., Moriguchi, A. and Maeda, K. (1997) In vivo transduction of cis element decoy against nuclear factor-κB binding site prevents myocardial infraction. Nat. Med. 3, 894–899.
[12] Morishita, R., Tomita, N., Kaneda, Y. and Ogihara, T. (2004) Molecular therapy to inhibit NFκB activation by transcription factor decoy oligonucleotide. Curr. Opin. Pharmacol. 4, 139–146.
[13] Higuchi, Y., Kawakami, S., Oka, M., Yamashita, F. and Hashida, M. (2006) Suppression of TNFα production in LPS induced liver failure mice after intravenous injection of cationic liposome/NFκB decoy complex. Pharmazie 61, 144–147.
[14] Ogushi, I., Iimuro, Y., Seki, E., Son, G., Hirano, T., Hada, T., Tsutsui, H., Nakanishi, K., Morishita, R., Kaneda, Y. and Fujimoto, J. (2003) Nuclear factor κB decoy oligonucleotides prevent endotoxin-induced fatal liver failure in a murine model. Hepatology 38, 335–344.
[15] Hirano, T., Fujimoto, J., Ueki, T., Yamamoto, H., Iwasaki, T., Morisita, R., Sawa, Y., Kaneda, Y., Takahashi, H. and Okamoto, E. (1998) Persistent gene expression in rat liver in vivo by repetitive transfections using HVJ-liposome. Gene Ther. 5, 459–464.
[16] Yoshida, M., Yamamoto, N., Uehara, T., Terao, R., Nitta, R., Harada, N., Hatano, E., Iimuro, Y. and Yamaoka, Y. (2002) Kupffer cell targeting by intraportal injection of the HVJ cationic liposome. Eur. Surg. Res. 34, 251–259.
[17] Kuiper, J., Brouwer, A., Knook, D.L. and van Berkel, T.J.C. (1994) Kupffer and sinusoidal endothelial cells in: The Liver: Biology and Pathobiology (Arias, I.M., Boyer, J.L., Fausto, N., Jakoby, W.B., Schachter, D.A. and Shafritz, D.A., Eds.), 3rd ed, pp. 791–818, Raven Press, NY.
[18] Dzau, V.J., Mann, M.J., Morishita, R. and Kaneda, Y. (1996) Fusigenic viral liposome for gene therapy in cardiovascular diseases. Proc. Natl. Acad. Sci. USA 93, 11421–11425.
[19] Hashida, M., Kawakami, S. and Yamashita, F. (2005) Lipid carrier systems for targeted drug and gene delivery. Chem. Pharm. Bull. 53, 871–880.
[20] Kawakami, S., Sato, A., Nishikawa, M., Yamashita, F. and Hashida, M. (2000) Mannose receptor-mediated gene transfer into macrophages using novel mannosylated cationic liposomes. Gene Ther. 7, 292–299.
[21] Kawakami, S., Hattori, Y., Lu, Y., Higuchi, Y., Yamashita, F. and Hashida, M. (2004) Effect of cationic charge on receptor-mediated transfection using mannosylated cationic liposome/plasmid DNA complexes following the intravenous administration in mice. Pharmazie 59, 405–408.
[22] Yamada, M., Nishikawa, M., Kawakami, S., Hattori, Y., Nakano, T., Yamashita, F. and Hashida, M. (2004) Tissue and intrahepatic distribution and subcellular localization of a mannosylated lipoplex after intravenous administration in mice. J. Control. Release 98, 157–167.
[23] Hattori, Y., Kawakami, S., Suzuki, S., Yamashita, F. and Hashida, M. (2004) Enhancement of immune responses by DNA vaccination through targeted gene delivery using mannosylated cationic liposome formulations following intravenous administration in mice. Biochem. Biophys. Res. Commun. 317, 992–999.
[24] Kawakami, S., Wong, J., Sato, A., Hattori, Y., Yamashita, F. and Hashida, M. (2000) Biodistribution characteristics of mannosylated, fucosylated, and galactosylated liposomes in mice. Biochim. Biophys. Acta 1524, 258–265.
[25] Hattori, Y., Suzuki, S., Kawakami, S., Yamashita, F. and Hashida, M. (2005) The role of dioleoylphosphatidylethanolamine (DOPE) in targeted gene delivery with mannosylated cationic liposomes via intravenous route. J. Control. Release 108, 484–495.

[26] Kawakami, S., Fumoto, S., Nishikawa, M., Yamashita, F. and Hashida, M. (2000) In vivo gene delivery to the liver using novel galactosylated cationic liposomes. Pharm. Res. 17, 306–313.
[27] Fumoto, S., Nakadori, F., Kawakami, S., Nishikawa, M., Yamashita, F. and Hashida, M. (2003) Analysis of hepatic disposition of galactosylated cationic liposome/plasmid DNA complexes in perfused rat liver. Pharm. Res. 20, 1452–1459.
[28] Kuiper, J. (1994) The Liver: Biology and Pathobiology, third ed, Raven Press, NY, p. 791.
[29] Yeeprae, W., Kawakami, S., Suzuki, S., Yamashita, F. and Hashida, M. (2006) Physicochemical and pharmacokinetic characteristics of cationic liposomes. Pharmazie 61, 102–105.
[30] Kawakami, S., Ito, Y., Fumoto, S., Yamashita, F. and Hashida, M. (2005) Enhanced gene expression in lung by a stabilized lipoplex using sodium chloride for complex formation. J. Gene Med. 7, 1526–1533.
[31] Higuchi, Y., Nishikawa, M., Kawakami, S., Yamashita, F. and Hashida, M. (2004) Uptake characteristics of mannosylated and fucosylated bovine serum albumin in primary cultured rat sinusoidal endothelial cells and Kupffer cells. Int. J. Pharm. 287, 147–154.
[32] Opanasopit, P., Nishikawa, M., Yamashita, F., Takakura, Y. and Hashida, M. (2001) Pharmacokinetic analysis of lectin-dependent biodistribution of fucosylated bovine serum albumin: a possible carrier for Kupffer cells. J. Drug Target. 9, 341–351.

Available online at www.sciencedirect.com
SCIENCE DIRECT®
Journal of Controlled Release 114 (2006) 69–77
journal of controlled release
www.elsevier.com/locate/jconrel

Biodistribution characteristics of amino acid dendrimers and their PEGylated derivatives after intravenous administration

Tatsuya Okuda [a,b], Shigeru Kawakami [a], Tadahiro Maeie [a], Takuro Niidome [c], Fumiyoshi Yamashita [a], Mitsuru Hashida [a,*]

[a] *Department of Drug Delivery Research, Graduate School of Pharmaceutical Sciences, Kyoto University, 46-29 Yoshida-Shimo-Adachi-cho, Sakyo-ku, Kyoto 606-8501, Japan*
[b] *Japan Association for the Advancement of Medical Equipment, 3-42-6 Hongo, Bunkyo-ku, Tokyo113-0033, Japan*
[c] *Department of Applied Chemistry, Faculty of Engineering, Kyushu University, 744 Motooka, Nishi-ku, Fukuoka 819-0395, Japan*

Received 14 March 2006; accepted 14 May 2006
Available online 23 May 2006

Abstract

In this study, we synthesized dendritic poly(L-lysine)s (DPKs), dendritic poly(L-ornithine)s (DPOs), which are constructed as novel amino acid dendrimers, and PEGylated KG6 (the sixth generation of DPKs), and evaluated the physicochemical properties and biodistribution characteristics of these dendrimers. The particle size of DPKs and DPOs was well controlled in the nanometer range. The zeta-potential of these dendrimers was slightly positive and this gradually increased in association with their generation. After intravenous administration to mice, all tested dendrimers cleared rapidly from blood flow and mainly accumulated in the liver and kidney. The hepatic and renal accumulation changed in a generation-dependent manner. In contrast, no significant distributional differences between same generation of DPK and DPO were observed, although the constituent amino acids, particle size, and zeta-potential were different. However, PEGylation of KG6 caused great changes in particle size, zeta-potential, blood retention and organ distribution in vivo, indicating that the PEGylation is applicable strategy to improve biodistribution characteristics of dendrimeric molecules. The information provided by this study will be helpful for the development of future drug delivery systems using amino acid dendrimers as safe drug carriers.

Keywords: Amino acid dendrimer; Biodistribution; Drug delivery system; Nano-carrier; PEGylation

1. Introduction

In spite of having excellent pharmacological effects, many drugs, especially most anticancer drugs, are limited in their clinical application due to a number of factors, including unfavorable biodistribution, serious toxicity, and poor water solubility. Therefore, in order to improve the biodistribution characteristics, suppress any harmful side effects, and enhance beneficial pharmacological effects, many research teams around the world are developing drug formulations, which can deliver pharmacologically active drugs to their target sites with high efficiency. In this field, several kinds of synthetic macromolecules have been developed and investigated as drug carriers [1–5]. Hence, the development of more functional drug carrier molecules is essential to attain a more targeted delivery of drugs.

To date, emulsions [6–8], liposomes [9–11], and polymeric micelles [12–14] have been developed as drug carriers. Since these carriers consist of amphiphilic molecules, they have a broad size distribution. In contrast, dendrimers have attracted great attention as far as biomedical application is concerned [15,16]. Dendrimers are unique highly branched spherical

Abbreviations: DPKs, dendritic poly(L-lysine)s; DPOs, dendritic poly(L-ornithine)s; KG6, the sixth generation of DPK; PAMAM, poly(amidoamine); Boc, *t*-butoxycarbonyl; DCHA, dicyclohexyl amine; HBTU, 2-(1*H*-benzotriazole-1-yl)-1,1,3,3-tetramethyluronium hexafluorophosphate; HOBt, 1-hydroxybenzotriazol; TFA, trifluoroacetic acid; DTPA, diethylenetriamine-*N*,*N*,*N*′,*N*″,*N*″-pentaacetic acid; MALDI TOF-MS, matrix-assisted time of flight mass spectrometry; DMF, *N*,*N*-dimethylformamide; PBS, phosphate-buffered saline; MWCO, molecular weight cut-off.

* Corresponding author. Tel.: +81 75 753 4525; fax: +81 75 753 4575.
E-mail address: hashidam@pharm.kyoto-u.ac.jp (M. Hashida).

0168-3659/$ - see front matter © 2006 Elsevier B.V. All rights reserved.
doi:10.1016/j.jconrel.2006.05.009

polymers with a narrow size distribution due to their distinctive method of synthesis (i.e., stepwise elongation of their generation). Monodispersed molecules like dendrimers would enable us to achieve more precise drug delivery. Therefore, dendrimers are potentially important candidates for the development of novel drug delivery systems. Poly(amidoamine) (PAMAM) dendrimer is a typical dendrimer. PAMAM dendrimers are commercially available macromolecules that can be used as carriers for plasmid DNA, antisense oligonucleotide and siRNA [17–21]. Moreover, PAMAM dendrimers are being investigated not only for gene therapy but also for drug delivery and bioimaging purposes [22,23]. However, Malik et al. have reported that PAMAM dendrimers exhibit generation-dependent cytotoxicity [24]. Furthermore, the mechanism of cell death induced by cationic PAMAM dendrimers has been reported by Kuo et al. [25]. Therefore, the work described here is intended to allow for the development of safer dendritic carrier molecules.

Dendritic poly(L-lysine)s (DPKs), which consist of amino acids, are also dendrimers that have different branch units compared with PAMAM-type dendrimers. Recently, we have reported that DPKs, especially its sixth generation (KG6), exhibit a high gene transfection ability in several kinds of cultivated cells without any significant cytotoxicity [26]. We also found that the KG6 had a protective effect against the degradation of plasmid DNA from endonucleases in blood in vivo, so that DPKs are expected to be good gene carrier not only in vitro but also in vivo [27]. DPKs can be synthesized with a well-defined structure and a precise number of surface amino groups per dendrimer. In addition, DPKs can easily alter their size and physicochemical properties by changing the constituent amino acid [28] and their surface amino groups can be modified by means of several functional groups, such as sugar chains, antibodies and so on. Therefore, amino acid dendrimers are important candidates for safer drug delivery systems.

When the newly developed material is used as a drug carrier, it is necessary to evaluate its own biodistribution characteristics. However, the in vivo disposition of amino acid dendrimers administered intravenously has not yet been investigated. In order to clarify the relationship between the physicochemical parameters and biodistribution characteristics of amino acid dendrimers, we synthesized several generations of DPKs and dendritic poly(L-ornithine)s (DPOs), which are composed of L-ornithine, and investigated their size, zeta-potential and disposition in mice after intravenous administration. Moreover, since there is no report in which the effect of PEGylation on the biodistribution characteristics of dendrimeric drug carriers has been discussed, we also prepared PEGylated KG6, and discuss them in the same way.

2. Materials and methods

2.1. Chemicals and instruments

Di-*t*-butyl dicarbonate (Boc_2O) was purchased from Peptide Institute, Inc. (Osaka, Japan). Organic solvents used in all synthesis procedures, lysine and ornithine monohydrochloride, ethylenediamine, hexamethylenediamine, and transaminase CII-test Wako were purchased from Wako Pure Chemical Industries, Ltd. (Osaka, Japan). The sixth generation of PAMAM dendrimer (PAMAM-G6) was purchased from SIGMA-ALDRICH Corporation (St. Louis, USA). Trifluoroacetic acid, dicyclohexyl amine (DCHA), and triethylamine were purchased from Nacalai Tesque, Inc. (Kyoto, Japan). The coupling reagents, 2-(1*H*-benzotriazole-1-yl)-1,1,3,3-tetramethyluronium hexafluorophosphate (HBTU) and 1-hydroxybenzotriazol (HOBt), were purchased from Novabiochem, Merck Ltd. (Tokyo, Japan). DTPA anhydride was purchased from Dojindo (Kumamoto, Japan). The $^{111}InCl_3$ was kindly provided by Nihon Medi-Physics Co. Ltd. (Hyogo, Japan). Mass spectra were obtained by matrix-assisted time of flight mass spectrometry (MALDI TOF-MS) using an Applied Biosystems, Voyager Linear DE instrument (Tokyo, Japan).

2.2. Synthesis of amino acid dendrimers

Lysine or ornithine monohydrochloride was dissolved in distilled water, and then Boc_2O in dioxane was added. The pH of the reaction mixture was adjusted to 8.0 or above by addition of 1 M NaOH. After overnight stirring at room temperature, dioxane was evaporated and the product was extracted with ethylacetate. The organic phase was washed three times with 10% citric acid and saturated NaCl, respectively, and then evaporated. *N*-Boc-protected lysine and ornithine were crystallized from petroleum ether with an equivalent molar ratio of DCHA. DPKs and DPOs were synthesized according to a method reported previously [26]. In brief, for the first generation synthesis, *N*-Boc-protected lysines or ornithines were coupled with diamines (hexamethylenediamine for DPKs or ethylenediamine for DPOs) in DMF by the HBTU-HOBt method [29], and then deprotection was performed by TFA treatment. For the synthesis of the second and higher generations, the coupling reaction between the amino group-free previous generation of dendrimers and *N*-Boc-protected lysines or ornithines was performed in DMF by the HBTU-HOBt method and, subsequently, Boc-groups were removed by TFA. We synthesized dendrimers up to the sixth generation by repetition of these coupling and deprotection procedures. The molecular weights of these synthesized dendrimers were measured by MALDI-TOF MS.

2.3. Evaluation of physicochemical properties of amino acid dendrimers

The fourth and further generations of dendrimers were suspended in PBS (pH 7.3) at a concentration of up to 5 mg/ml, and then their particle size and zeta-potential were measured by Zetasizer Nano ZS (Malvern Instruments Ltd., United Kingdom).

2.4. Radiolabeling of amino acid dendrimers

For the biodistribution experiments, each generation of amino acid dendrimers was radiolabeled with ^{111}In using the

bifunctional chelating agent, DTPA anhydride, according to the method of Hnatowich et al. [30]. This radiolabeling method is suitable for examining the biodistribution of macromolecules from plasma to various tissues because the radioactive metabolites, if produced after cellular uptake, are retained within the cells where the uptake takes place [31,32]. In brief, the amino acid dendrimer was dissolved in 20 mM borate buffer (pH 9.8) and DTPA anhydride in dimethyl sulfoxide was added at the molar ratio of 1:1. After mixing for 1 h at room temperature, the reaction mixture was purified by ultrafiltration using a VIVASPIN-20 (MWCO 3000 for the fourth generation or 5000 for the fifth and sixth generations). The purified DTPA-labeled dendrimer was then lyophilized, and the DTPA-labeled dendrimer solution was dissolved in 100 mM sodium citrate buffer (pH 5.5) at a concentration of 2 mg/ml. Twenty microliters $^{111}InCl_3$ solution was mixed with an equivalent volume of 100 mM sodium citrate buffer, and the mixture was allowed to stand for a few minutes. Then, 40 μl DTPA-labeled dendrimer solution was added and mixed well. After standing for 30 min at room temperature, the mixture was purified by gel filtration chromatography using a PD-10 column and eluted with sodium citrate buffer. The appropriate fractions were selected based on their radioactivity and concentrated by ultrafiltration using a VIVASPIN-20.

2.5. PEGylation of KG6

In order to prevent steric hindrance by PEG chains on the surface of dendrimer, the reaction between KG6 and DTPA anhydride was performed by the method described above before PEGylation. The DTPA-labeled KG6 was dissolved in borate buffer and reacted with PEG-NHS (Mw: 5000) at 4 °C. After overnight incubation, the reaction mixture was subjected to ultrafiltration using a VIVASPIN (MWCO 100,000). The degree of modification of the surface primary amino groups by PEG-NHS was evaluated by the barium–iodine method [33].

2.6. Animals

Male ddY mice (5 weeks old, 25–27 g) were purchased from Shizuoka Agricultural Co-Operative Association for Laboratory Animals (Shizuoka, Japan). Animals were maintained under conventional housing conditions. All animal experiments were performed according to the Guidelines for Animal Experimentation at Kyoto University.

2.7. Biodistribution experiment

^{111}In-labeled dendrimer was dissolved in saline, and the concentration of dendrimer was adjusted by addition of non-radiolabeled dendrimer to the solution. The ^{111}In-labeled dendrimer solution was administered via the tail vein to 5-week-old ddY mice at a dose of 1 mg/kg. At an appropriate time interval after intravenous injection, blood was collected from the vena cava under ether anesthesia and the mice were then sacrificed. The liver, kidneys, spleen, heart, and lungs were removed, rinsed with saline, blotted dry, and weighed. The collected blood was centrifuged for 5 min at 2000×*g* to obtain plasma. Samples of the collected organs and 100 μl plasma were transferred to counting tubes, and the radioactivity of each sample was measured using a gamma counter.

2.8. In vivo cytotoxicity analysis

The sixth generation of DPK and PAMAM dendrimer was administered via tail vein to 5-week-old ddY mice at three doses (1 mg/kg, 5 mg/kg, 10 mg/kg). Blood was collected at 24 h after administration. Serum was prepared by incubation of collected blood for 30 min at room temperature and centrifugation at 6000×*g* for 20 min at 4 °C. The serum glutamic pyruvic

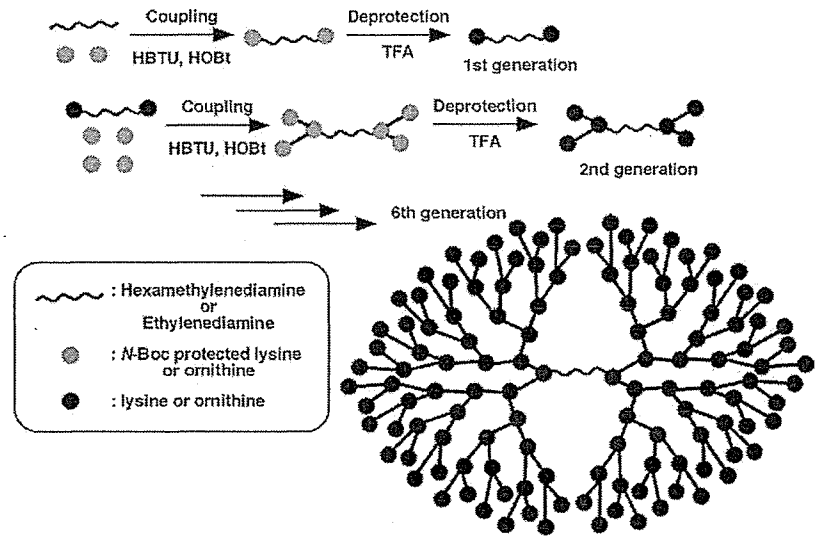

Fig. 1. Structure and synthetic route of amino acid dendrimers.

transaminase (GPT) activities were measured by using commercial kit (Transaminase CII-test Wako).

2.9. Statistical analysis

Statistical analysis was performed using Student's paired *t*-test for two groups. Multiple comparisons among different generations were made by Tukey–Kramer test or ANOVA with Dunnett's mean test. $P<0.05$ was considered to be indicative of statistical significance.

3. Results

3.1. Synthesis of amino acid dendrimers

The structures of DPKs and DPOs, a novel type of amino acid dendrimer, are shown in Fig. 1. DPKs and DPOs were synthesized from hexamethylenediamine or ethylenediamine as the initiator core, respectively. The first generation of each of the amino acid dendrimers was synthesized by coupling *N*-Boc-protected lysine or ornithine to the core molecule by the HBTU-HOBt method [29]. The second to sixth generations of each of the amino acid dendrimers were obtained by repetition of coupling and deprotection with TFA. After every coupling step, the amino acid dendrimers were purified by extraction or gel chromatography. The first to sixth generations of DPKs and DPOs were named KG1 to KG6 and OG1 to OG6, respectively. The final preparations of the fourth and further dendrimers were identified by MALDI TOF-MS (data not shown).

3.2. Physicochemical properties of amino acid dendrimers

The physicochemical properties of amino acid dendrimers were analyzed by a Zetasizer Nano ZS (Table 1). The mean diameter of KG4 to KG6 was about 3.41, 4.70, and 5.85 nm, respectively. On the other hand, the mean particle size of OG4 to OG6 was about 3.20, 3.96, and 5.22 nm, respectively. The particle size of each series of dendrimers increased gradually depending on their generation. All amino acid dendrimers subjected to zeta-potential analysis had a slightly positive potential and their surface charge gradually increased with their generation. DPKs were slightly larger with a higher zeta-potential than DPOs of the same generation.

Table 1
Physicochemical properties of amino acid dendrimers in PBS

	Molecular Weight	Number of $-NH_2$ groups	Particle size (nm)	Zeta-potential (mV)
KG4	3962	32	3.41±0.13	14.86±0.73
KG5	8065	64	4.70±0.04	17.31±4.54
KG6	16,269	128	5.85±0.06	19.77±0.30
OG4	3485	32	3.20±0.06	6.52±0.58
OG5	7139	64	3.96±0.08	9.49±0.33
OG6	14,446	128	5.22±0.03	9.33±0.46

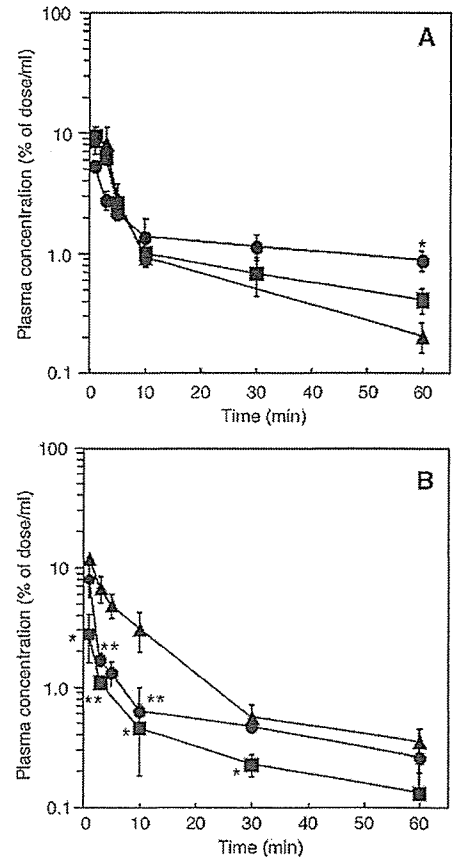

Fig. 2. Plasma concentration of ^{111}In-labeled DPKs (A) and DPOs (B) after intravenous administration to mice at a dose of 1 mg/kg. The fourth (▲), fifth (■), and sixth (●) generation of amino acid dendrimers were subjected to biodistribution experiments. Each value represents the mean±S.D. of three experiments. Statistically significant differences compared with the fourth generation (*$P<0.05$; **$P<0.01$) or the fifth generation (†$P<0.05$; ††$P<0.01$).

3.3. Plasma concentration of ^{111}In-labeled amino acid dendrimers

Fig. 2 shows the plasma concentration profiles of ^{111}In-labeled DPKs (A) and DPOs (B) after intravenous injection into mice up to 60 min. All amino acid dendrimers were rapidly eliminated from blood circulation within a few minutes, indicating that the amino acid dendrimer rapidly accumulated in some organs or was excreted into urine and feces. Although the particle size (generation), zeta-potential, and the constituent amino acids were different, no significant differences in the blood concentration profiles of the ^{111}In-labeled amino acid dendrimers were observed.

3.4. Tissue distribution of ^{111}In-labeled amino acid dendrimers

The biodistribution characteristics of the amino acid dendrimers were evaluated up to 60 min post-intravenous injection into mice by measuring the radioactivity in the liver, kidney, spleen, heart, lung, and urine. Regardless of the constituent amino acid and its generation, most of the amino

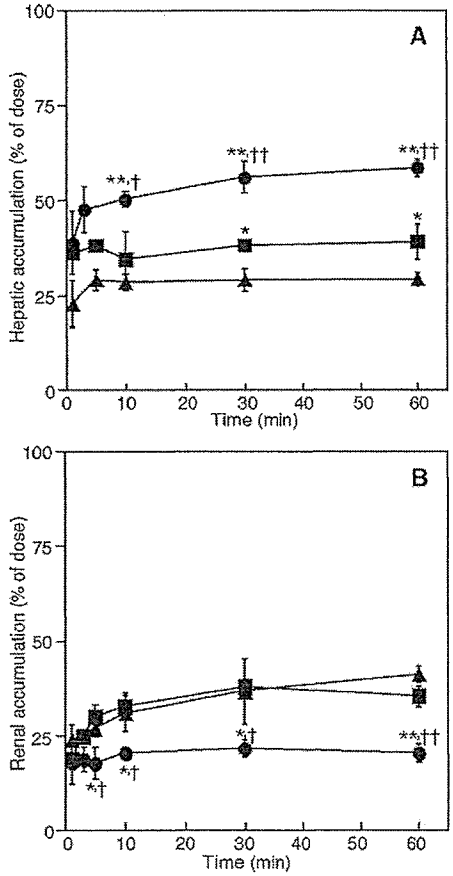

Fig. 3. Hepatic (A) and renal (B) accumulation of ^{111}In-labeled DPKs after intravenous administration to mice at a dose of 1 mg/kg. The fourth (▲), fifth (■), and sixth (●) generation of DPKs were subjected to biodistribution experiments. Each value represents the mean±S.D. of three experiments. Statistically significant differences compared with the fourth generation (*P<0.05; **P<0.01) or the fifth generation (†P<0.05; ††P<0.01).

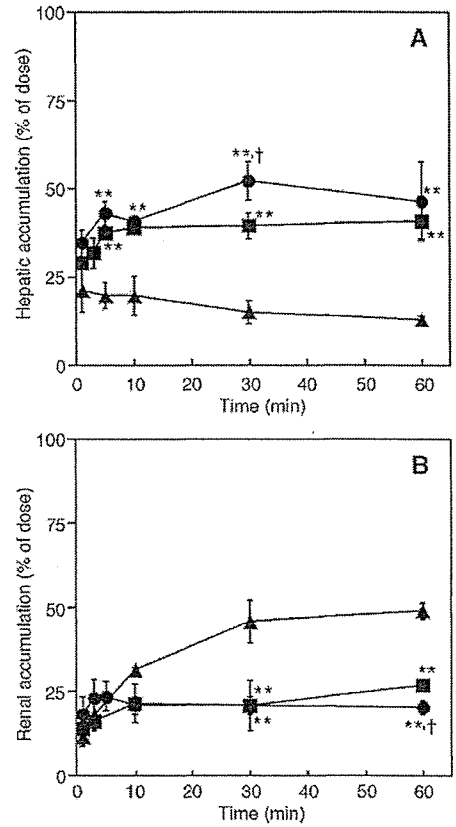

Fig. 4. Hepatic (A) and renal (B) accumulation of ^{111}In-labeled DPOs after intravenous administration to mice at a dose of 1 mg/kg. The fourth (▲), fifth (■), and sixth (●) generation of DPOs were subjected to biodistribution experiments. Each value represents the mean±S.D. of three experiments. Statistically significant differences compared with the fourth generation (*P<0.05; **P<0.01) or the fifth generation (†P<0.05; ††P<0.01).

acid dendrimers were recovered from the liver and kidney. The hepatic and renal accumulation profiles of DPKs and DPOs are shown in Figs. 3 and 4, respectively. The hepatic disposition of both DPKs and DPOs gradually increased in a generation-dependent manner (Figs. 3A and 4A). However, the higher the generation, the lower the renal accumulation of dendrimer (Figs. 3B and 4B). Also, no significant difference between the same generation of DPK and DPO was observed as far as both hepatic and renal accumulation were concerned. In contrast, all dendrimers investigated were virtually never detected in the spleen, heart, lung, and urine (data not shown).

3.5. *In vivo cytotoxicity of dendrimers*

To investigate in vivo cytotoxicity of KG6 and PAMAM dendrimer, serum GPT activity was measured at 24 h post-administration (Fig. 5). As a result, the serum GPT activities of KG6- or PAMAM-G6-treated mice were slightly increased with dose-dependent manner compared with saline treatment group. However, these values were within normal levels,

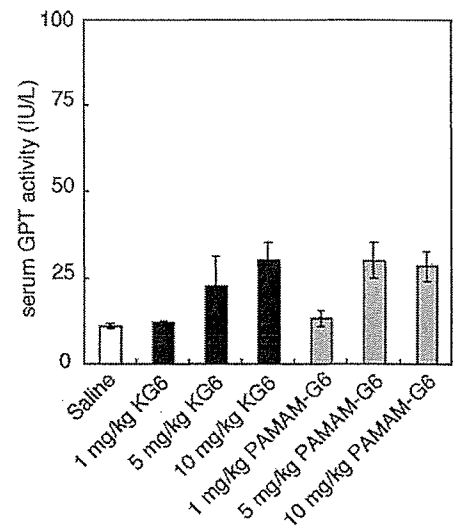

Fig. 5. The serum GPT activities at 24 h after intravenous administration of KG6 and PAMAM-G6 at three doses (1 mg/kg, 5 mg/kg, 10 mg/kg). Each value represents the mean±S.D. of three experiments. Statistically significant differences (*P<0.05) between saline treatment group and three doses of KG6 or PAMAM-G6 were analyzed by ANOVA with Dunnett's multiple comparison of means test.

Table 2
Physicochemical properties of PEGylated KG6 in PBS

	Number of PEG_{5000} [a]	Number of $-NH_2$ groups [b]	Particle size (nm)	Zeta-potential (mV)
KG6	0	128	5.85±0.06	19.77±0.30
PEG-KG6	76.2	51.8	16.92±0.13	−6.51±0.18

[a] The number of PEG_{5000} was determined by the barium–iodine method.
[b] The number of surface amino groups was determined by subtracting the result of the barium–iodine method from the number of native KG6's surface amino groups.

suggesting that KG6 and PAMAM-G6 showed no significant acute hepatic damages even at the dose of 10 mg/kg.

3.6. Surface modification of KG6 with polyethylene glycol chain

In order to investigate the influence of surface modification of the amino acid dendrimer in terms of its biodistribution, PEGylation of KG6 was performed. The degree of modification of PEGylated-KG6 was evaluated by the barium–iodine method [33], and found to be 59.5%. The particle size and zeta-potential of PEGylated-KG6 were measured (Table 2). The particle size increased about 2.5-fold compared with intact KG6, and the zeta-potential shifted from positive to slightly negative.

3.7. Plasma concentration of ^{111}In-labeled PEGylated KG6

PEGylated-KG6 was subjected to a biodistribution experiment identical to that for other surface non-modified amino acid dendrimers. The plasma concentration profile of intravenously administered ^{111}In-labeled PEGylated-KG6 up to 60 min is shown in Fig. 6A. The retention time in the blood was dramatically enhanced by PEGylation of KG6. Furthermore, about 20% of the injected dose was recovered from plasma even at 24 h after intravenous injection (Fig. 6B).

3.8. Tissue distribution of ^{111}In-labeled PEGylated KG6

PEGylated-KG6 also scarcely accumulated in the spleen, heart, lung, and urine like other intact amino acid dendrimers. The hepatic accumulation of PEGylated-KG6 was significantly lower compared with KG6 (Fig. 7A). On the other hand, no renal accumulation of PEGylated-KG6 was detected (Fig. 7B).

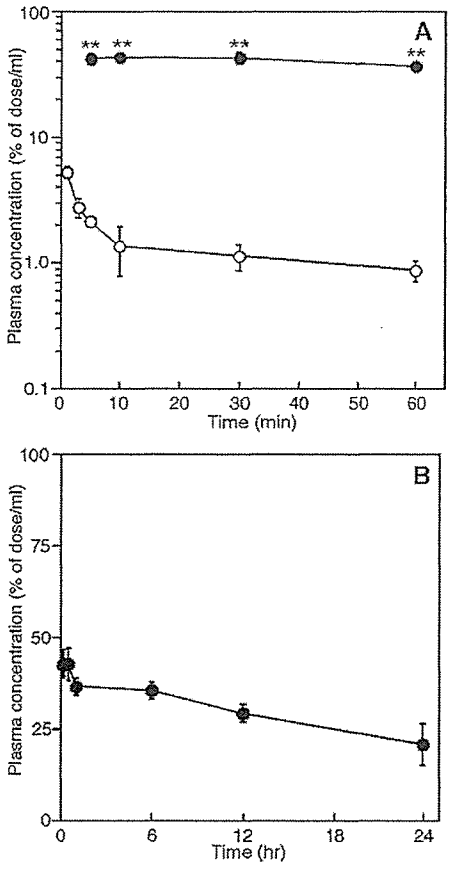

Fig. 6. The short-term (A) and long-term (B) plasma concentration profiles of ^{111}In-labeled PEGylated KG6 after intravenous administration to mice at a dose of 1 mg/kg. Each value represents the mean±S.D. of three experiments. Closed and open circles represent plasma concentration profiles of PEGylated KG6 and intact KG6, respectively. Statistically significant differences (*$P<0.05$; **$P<0.01$) between PEGylated KG6 and intact KG6 at each time point.

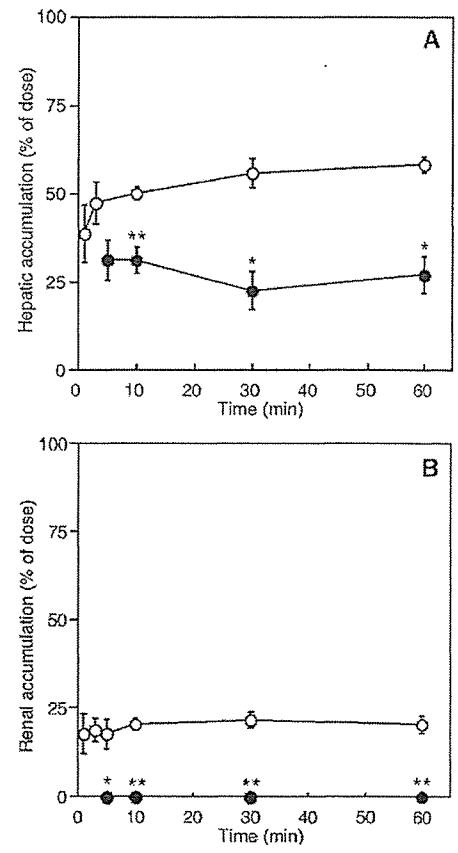

Fig. 7. Hepatic (A) and renal (B) accumulation of ^{111}In-labeled PEGylated KG6 after intravenous administration to mice at a dose of 1 mg/kg. Each value represents the mean±S.D. of three experiments. Closed and open circle represent biodistribution profiles of PEGylated KG6 and intact KG6, respectively. Statistically significant differences (*$P<0.05$; **$P<0.01$) between PEGylated KG6 and intact KG6 at each time point.

4. Discussion

Dendrimers can be synthesized with well-controlled size in nanometer properties. We easily obtained derivatives of amino acid dendrimers that had different particle sizes, zeta-potentials, and physicochemical and biological properties by altering the constituent amino acid and/or modifying surface amino groups with several functional groups [28]. Furthermore, our previous report demonstrated that DPKs are important candidates for safer carriers [26]. Therefore, we expect amino acid dendrimers to be promising basic materials for the development of safer carrier systems in the field of nano-medicine and focused on DPKs. In addition to DPKs, DPOs and PEGylated KG6 were synthesized to investigate the effect of generation, and physicochemical properties on their distribution after intravenous administration.

Since physicochemical properties, such as particle size and zeta-potential, are important factors controlling the biodistribution characteristics [34], we measured these two parameters. Both DPKs and DPOs could be synthesized with well-controlled size in nanometer properties (Table 1). The DPOs were smaller in size than the same generation of DPKs. This observation agrees with the fact that the side chain of ornithine is shorter than that of lysine. The zeta-potentials of all amino acid dendrimers examined in this study were slightly positive and increased in a generation-dependent manner. However, the zeta-potential of DPOs was lower compared with same generation of DPKs (Table 1). The reason for this difference in zeta-potential may be due to the fact that the protonation of surface amino group may be inhibited to suppress the charge repulsion caused by the high density of surface primary amino groups of DPOs, which have a more compact structure compared with the same generation of DPKs.

As shown in Figs. 2–4, all dendrimers investigated were rapidly eliminated from the blood and accumulated in mainly the liver and kidney. Unexpectedly, OG4 showed, however, substantially slower clearance from blood stream in the initial elimination phase compared with OG5 and OG6 (Fig. 2B). Maybe this unforeseen behavior of OG4 is due to its lower accumulation than the fifth and sixth generation of DPOs into liver and kidney in the early phase (Fig. 4). Although lung and spleen are a part of reticulo-endothelial system (RES) known to be involved in clearing macromolecule, no significant accumulation was observed not only in the heart and urine but also in lung and spleen. This reason why is mostly due to very rapid elimination of intravenously injected DPKs and DPOs from the blood stream (Fig. 2). The amount of hepatic accumulation increased in a generation-dependent manner (Figs. 3A and 4A). This increment in hepatically distributed dendrimer is caused by an increase in the surface positive charge in parallel with the generation increment. The kidney plays an important role in the clearance of macromolecules circulating in the bloodstream. Macromolecules with a molecular weight less than 50,000 (approximately 6 nm in diameter) are susceptible to glomerular filtration and are excreted in the urine [35]. Interestingly, although all the amino acid dendrimers used in this study have a subliminal molecular weight of glomerular filtration (Table 1), the dendrimers accumulated in kidney without any significant urinary excretion (Figs. 3B and 4B). We previously reported that cationic macromolecules, such as diethylaminoethyl-dextran (DEAE-dextran) and cationized BSA, are taken up by kidney from the capillary side based on electrostatic interactions and are distributed to both the medulla and cortex region [36]. The same phenomenon might have been caused by the highly concentrated positive charge on the surface of the amino acid dendrimers.

Since intravenously administered amino acid dendrimers rapidly accumulated into the liver, it was a concern that hepatically accumulated dendrimers might cause acute hepatic damages. Therefore, the serum GPT activity was measured at 24 h after administration. The serum GPT activities of KG6- or PAMAM-G6-treated mice were dose-dependently increased (Fig. 5). However, these values were within normal levels. Moreover, because the serum GPT level reached at several hundreds or thousands IU/L when the acute hepatic damages were induced by CCl_4-treatment, serum GPT activities observed at 24 h post-administration were considered to be significantly lower levels even at the dose of 10 mg/kg. In this experiment, the sixth generation of PAMAM dendrimer also showed no significant hepatic toxicity. Hence, both KG6 and PAMAM-G6 might have no acute hepatic toxicity. However, since the in vitro cytotoxicity of PAMAM dendrimers have been reported [24,25], we are convinced that amino acid dendrimers are safer than PAMAM dendrimers.

Polyethylene glycol (PEG), which is a biocompatible material, could improve the biodistribution by suppressing any unfavorable non-specific interaction with biomolecules. In order to confirm the effect of PEGylation on the disposition of amino acid dendrimers, PEGylation of KG6 was performed and the biodistribution characteristics of PEGylated-KG6 were evaluated. The particle size increased about 2.5-fold compared with intact KG6 and the zeta-potential shifted from positive to slightly negative following surface modification of KG6 with PEG chains (Table 2). As shown in Fig. 6, PEGylation of KG6 substantially enhanced blood retention, compared with that of intact KG6. Furthermore, the PEGylation reduced hepatic accumulation and almost completely abolished renal accumulation (Fig. 6). These results well agree with reports that PEGylation of drug carriers such as liposome and other polymer could improve their biodistribution characteristics by reducing non-specific interaction with biomolecules. This finding is strongly suggesting that PEGylation is also able to improve the biodistribution properties of the dendrimeric drug carriers such as amino acid dendrimers.

In conclusion, we synthesized DPKs, DPOs, and PEGylated KG6 and evaluated the effect of generation and physicochemical properties on biodistribution after intravenous administration. Although each amino acid dendrimer has a different particle size and zeta-potential at the same generation, no significant difference in the biodistribution characteristics of the amino acid dendrimers was observed. However, the hepatic and

renal accumulation was altered in a generation-dependent manner. Moreover, PEGylation of the dendrimers dramatically changed their disposition in vivo, suggesting that the PEGylation is also useful strategy to improve biodistribution characteristics of dendrimeric drug carriers. Our findings should be helpful for the exploitation of amino acid dendrimers as future drug delivery carriers.

Acknowledgements

This work was supported in part by Grants-in-Aid for Scientific Research from the Ministry of Education, Culture, Sports, Science, and Technology of Japan, and by the Health and Labour Sciences Research Grants for Research on Advanced Medical Technology from the Ministry of Health, Labour and Welfare of Japan.

We acknowledge the operation of the MALDI TOF-MS by Mr. Ryosuke Kurihara in the Department of Applied Chemistry, Faculty of Engineering, Kyushu University, Fukuoka, Japan.

References

[1] T. Etrych, M. Jelinkova, B. Rihova, K. Ulbrich, New HPMA copolymers containing doxorubicin bound via pH-sensitive linkage: synthesis and preliminary in vitro and in vivo biological properties, J. Control. Release 73 (2001) 89–102.
[2] M. Ozeki, T. Ishii, Y. Hirano, Y. Tabata, Controlled release of hepatocyte growth factor from gelatin hydrogels based on hydrogel degradation, J. Drug Target. 9 (2001) 461–471.
[3] T. Kushibiki, K. Matsumoto, T. Nakamura, Y. Tabata, Suppression of the progress of disseminated pancreatic cancer cells by NK4 plasmid DNA released from cationized gelatin microspheres, Pharm. Res. 21 (2004) 1109–1118.
[4] M. Higaki, T. Ishihara, N. Izumo, M. Takatsu, Y. Mizushima, Treatment of experimental arthritis with poly(D,L-lactic/glycolic acid) nanoparticles encapsulating betamethasone sodium phosphate, Ann. Rheum. Dis. 64 (2005) 1132–1136.
[5] T. Takahashi, Y. Yamada, K. Kataoka, Y. Nagasaki, Preparation of a novel PEG-clay hybrid as a DDS material: dispersion stability and sustained release profiles, J. Control. Release 107 (2005) 408–416.
[6] P.J. Stevens, R.J. Lee, A folate receptor-targeted emulsion formulation for paclitaxel, Anticancer Res. 23 (2003) 4927–4931.
[7] J. Han, S.S. Davis, C. Papandreou, C.D. Melia, C. Washington, Design and evaluation of an emulsion vehicle for paclitaxel: I. Physicochemical properties and plasma stability, Pharm. Res. 21 (2004) 1573–1580.
[8] W. Yeepare, S. Kawakami, Y. Higuchi, F. Yamashita, M. Hashida, Biodistribution characteristics of mannosylated and fucosylated O/W emulsions in mice, J. Drug Target. 13 (2005) 1–9.
[9] H. Harashima, S. Iida, Y. Urakami, M. Tsuchihashi, H. Kiwada, Optimization of antitumor effect of liposomally encapsulated doxorubicin based on simulations by pharmacokinetic/pharmacodynamic modeling, J. Control. Release 61 (1999) 93–106.
[10] S. Kawakami, J. Wong, A. Sato, Y. Hattori, F. Yamashita, M. Hashida, Biodistribution characteristics of mannosylated, fucosylated, and galactosylated liposomes in mice, Biochim. Biophys. Acta 1524 (2000) 258–265.
[11] X. Guo, F.C. Szoka Jr., Steric stabilization of fusogenic liposomes by a low-pH sensitive PEG-diortho ester-lipid conjugate, Bioconjug. Chem. 12 (2001) 291–300.
[12] A.N. Lukyanov, V.P. Torchilin, Micelles from lipid derivatives of water-soluble polymers as delivery systems for poorly soluble drugs, Adv. Drug Deliv. Rev. 56 (2004) 1273–1289.
[13] Y. Bae, N. Nishiyama, S. Fukushima, H. Koyama, M. Yasuhiro, K. Kataoka, Preparation and biological characterization of polymeric micelle drug carriers with intracellular pH-triggered drug release property: tumor permeability, controlled subcellular drug distribution, and enhanced in vivo antitumor efficacy, Bioconjug. Chem. 16 (2005) 122–130.
[14] S. Kawakami, P. Opanasopit, M. Yokoyama, N. Chansri, T. Yamamoto, T. Okano, F. Yamashita, M. Hashida, Biodistribution characteristics of all-trans retinoic acid incorporated in liposomes and polymeric micelles following intravenous administration, J. Pharm. Sci. 94 (2005) 2606–2615.
[15] R. Esfand, D.A. Tomalia, Poly(amidoamine) (PAMAM) dendrimers: from biomimicry to drug delivery and biomedical applications, Drug Discov. Today 6 (2001) 427–436.
[16] S.E. Stibira, H. Frey, R. Haag, Dendritic polymers in biomedical applications: from potential to clinical use in diagnostics and therapy, Angew. Chem., Int. Ed. 41 (2002) 1329–1334.
[17] H. Yoo, P. Sazani, R.L. Juliano, PAMAM dendrimers as delivery agents for antisense oligonucleotides, Pharm. Res. 16 (1999) 1799–1804.
[18] H. Yoo, R.L. Juliano, Enhanced delivery of antisense oligonucleotides with fluorophore-conjugated PAMAM dendrimers, Nucleic Acids Res. 28 (2000) 4225–4231.
[19] J.S. Choi, K. Nam, J.Y. Park, J.B. Kim, J.K. Lee, J.S. Park, Enhanced transfection efficiency of PAMAM dendrimer by surface modification with L-arginine, J. Control. Release 99 (2004) 445–456.
[20] K. Wada, H. Arima, T. Tsutsumi, F. Hirayama, K. Uekama, Enhancing effects of galactosylated dendrimer/alpha-cyclodextrin conjugates on gene transfer efficiency, Biol. Pharm. Bull. 28 (2005) 500–505.
[21] H. Kang, R. Delong, M.H. Fisher, R.L. Juliano, Tat-conjugated PAMAM dendrimers as delivery agents for antisense and siRNA oligonucleotides, Pharm. Res. 22 (2005) 2099–2106.
[22] H. Kobayashi, S. Kawamoto, R.A. Star, T.A. Waldmann, Y. Tagaya, M.W. Brechbiel, Micro-magnetic resonance lymphangiography in mice using a novel dendrimer-based magnetic resonance imaging contrast agent, Cancer Res. 63 (2003) 271–276.
[23] H. Kobayashi, S.K. Jo, S. Kawamoto, H. Yasuda, X. Hu, M.V. Knopp, M. W. Brechbiel, P.L. Choyke, R.A. Star, Polyamine dendrimer-based MRI contrast agents for functional kidney imaging to diagnose acute renal failure, J. Magn. Reson. Imaging 20 (2004) 512–518.
[24] N. Malik, R. Wiwattanapatapee, R. Klopsch, K. Lorenz, H. Frey, J.W. Weener, E.W. Meijer, W. Paulus, R. Duncan, Dendrimers: relationship between structure and biocompatibility in vitro, and preliminary studies on the biodistribution of ^{125}I-labelled polyamidoamine dendrimers in vivo, J. Control. Release 65 (2000) 133–148.
[25] J.H. Kuo, M.S. Jan, H.W. Chiu, Mechanism of cell death induced by cationic dendrimers in RAW 264.7 murine macrophage-like cells, J. Pharm. Pharmacol. 57 (2005) 489–495.
[26] M. Ohsaki, T. Okuda, A. Wada, T. Hirayama, T. Niidome, H. Aoyagi, In vitro gene transfection using dendritic poly(L-lysine), Bioconjug. Chem. 13 (2002) 510–517.
[27] T. Kawano, T. Okuda, H. Aoyagi, T. Niidome, Long circulation of intravenously administered plasmid DNA delivered with dendritic poly(L-lysine) in the blood flow, J. Control. Release 99 (2004) 329–337.
[28] T. Okuda, A. Sugiyama, T. Niidome, H. Aoyagi, Characters of dendritic poly(L-lysine) analogues with the terminal lysines replaced with arginines and histidines as gene carriers in vitro, Biomaterials 25 (2004) 537–544.
[29] C.G. Fields, D.H. Lloyd, R.L. Macdonald, K.M. Otteson, R.L. Noble, HBTU activation for automated Fmoc solid phase peptide synthesis, Pept. Res. 4 (1991) 95–101.
[30] D. Hnatowich, W.W. Layne, R.L. Childs, The preparation and labeling of DTPA-coupled albumin, J. Appl. Radiat. Isot. 12 (1982) 327–332.
[31] J.R. Duncan, M.J. Welch, Intracellular metabolilsm of indium-111-DTPA-labeled receptor targeted proteins, J. Nucl. Med. 34 (1993) 1728–1738.
[32] F. Staud, M. Nishikawa, K. Morimoto, Y. Takakura, M. Hashida, Disposition of radioactivity after injection of liver-targeted proteins

labeled with ^{111}In or ^{125}I. Effect of labeling on distribution and excretion of radioactivity in rats, J. Pharm. Sci. 88 (1999) 577–585.
[33] B. Skoog, Determination of polyethylene glycols 4000 and 6000 in plasma protein preparations, Vox Sang. 37 (1979) 345–349.
[34] Y. Takakura, M. Hashida, Macromolecular carrier systems for targeted drug delivery: pharmacokinetic considerations on biodistribution, Pharm. Res. 13 (1996) 820–830.
[35] B.M. Brenner, T.H. Hostetter, H.D. Humes, Glomerular permselectivity: barrier function based on discrimination of molecular size and charge, Am. J. Physiol. 234 (1978) F455–F460.
[36] K. Mihara, M. Mori, T. Hojo, Y. Takakura, H. Sezaki, M. Hashida, Disposition characteristics of model macromolecules in the perfused rat kidney, Biol. Pharm. Bull. 16 (1993) 158–162.

THE JOURNAL OF GENE MEDICINE
J Gene Med 2006; 8: 824–834.
Published online 20 April 2006 in Wiley InterScience (www.interscience.wiley.com) **DOI:** 10.1002/jgm.910

RESEARCH ARTICLE

Enhanced DNA vaccine potency by mannosylated lipoplex after intraperitoneal administration

Yoshiyuki Hattori
Shigeru Kawakami
Yan Lu
Kazumi Nakamura
Fumiyoshi Yamashita
Mitsuru Hashida*

Department of Drug Delivery Research, Graduate School of Pharmaceutical Sciences, Kyoto University, Sakyo-ku, Kyoto 606-8501, Japan

*Correspondence to:
Mitsuru Hashida, Department of Drug Delivery Research, Graduate School of Pharmaceutical Sciences, Kyoto University, Sakyo-ku, Kyoto 606-8501, Japan. E-mail: hashidam@pharm.kyoto-u.ac.jp

Received: 15 December 2005
Revised: 31 January 2006
Accepted: 1 February 2006

Abstract

Background Here we describe a novel DNA vaccine formulation that can enhance cytotoxic T lymphocyte (CTL) activity through efficient gene delivery to dendritic cells (DCs) by mannose receptor-mediated endocytosis.

Methods Ovalbumin (OVA) was selected as a model antigen for vaccination; accordingly, OVA-encoding pDNA (pCMV-OVA) was constructed to evaluate DNA vaccination. Mannosylated cationic liposomes (Man-liposomes) were prepared using cholesten-5-yloxy-*N*-{4-[(1-imino-2-D-thiomannosylethyl)amino]butyl}formamide (Man-C4-Chol) with cationic lipid. The potency of the mannosylated liposome/pCMV-OVA complex (Man-lipoplex) was evaluated by measuring OVA mRNA in $CD11c^+$ cells, CTL activity, and the OVA-specific anti-tumor effect after *in vivo* administration.

Results An *in vitro* study using DC2.4 cells demonstrated that Man-liposomes could transfect pCMV-OVA more efficiently than cationic liposomes via mannose receptor-mediated endocytosis. *In vivo* studies revealed that the Man-lipoplex exhibited higher OVA mRNA expression in $CD11c^+$ cells in the spleen and peritoneal cavity and provided a stronger OVA-specific CTL response than intraperitoneal (i.p.) administration of the conventional lipoplex and intramuscular (i.m.) administration of naked pCMV-OVA, the standard protocol for DNA vaccination. Pre-immunization with the Man-lipoplex provided much better OVA-specific anti-tumor effect than naked pCMV-OVA via the i.m. route.

Conclusions These results suggested that *in vivo* active targeting of DNA vaccine to DCs with Man-lipoplex might prove useful for the rational design of DNA vaccine. Copyright © 2006 John Wiley & Sons, Ltd.

Keywords gene therapy; DNA vaccine; mannosylated liposomes; non-viral vectors

Introduction

DNA vaccine, plasmid DNA (pDNA)-encoding antigen from a pathogen, is of great interest in gene therapy as a means of immunotherapy against refractory diseases such as cancer and viral infections because the administration of naked pDNA-encoding antigen proteins induces not only an antibody response, but also a potent cytotoxic T lymphocyte (CTL) response in animal models [1–3]. Recent immunological studies have demonstrated that gene transfection and subsequent activation of antigen-presenting cells (APCs), dendritic cells (DCs) and macrophages are important for efficient DNA

vaccine therapy [4–6]. Although some clinical trials involving melanoma, human imuunodeficiency virus, and HCV have been performed using topical administration of naked pDNA [7–9], the results are not good enough for clinical therapy. In order to overcome this problem, it is important to develop gene delivery carriers for *in vivo* APC-selective gene transfection.

In spite of the high transfection efficiency of viral vectors, they still need to be improved from the point of view of safety issues [10–12]. The use of non-viral vectors is one of the possible approaches for *in vivo* gene delivery because they are free from some of the risks inherent in these systems. Furthermore, the characteristics of non-viral vectors can be more easily modified than those of viral vectors. To achieve targeted gene delivery, a number of receptor-mediated gene delivery systems have been developed [13–16] including our carriers [17–22]. As far as *in vivo* selective gene delivery to APCs is concerned, mannose has been shown to be a promising ligand to target APCs because these cells have a large number of mannose receptors.

Recently, we have developed several types of macromolecular [18] and particulate [22,23] gene carriers for macrophage-selective gene transfection *in vivo*. Among them, cationic liposomes containing cholesten-5-yloxy-*N*-{4-[(1-imino-2-D-thiomannosylethyl)amino]butyl} formamide (Man-C4-Chol) are some of the most interesting potential gene transfection carriers [22,23] that can be efficiently recognized by mannose receptors on macrophages in liver. Man-C4-Chol exhibits bifunctional properties, i.e., an imino group for binding to pDNA via electrostatic interaction and a mannose residue for the cell-surface receptors in APCs [22]. Therefore, a high density of mannose residues can be provided on the liposome surface without affecting the binding of the cationic liposomes to pDNA. More recently, we have demonstrated that intravenously administrated pCMV-OVA complexed with mannosylated liposomes (Man-lipoplex) enhances MHC class I antigen presentation, but no measurable CTL response was observed [24], suggesting that not only cell-selective gene transfection but also enhanced transfection efficiency in DCs is needed for gene therapy.

Intraperitoneal (i.p.) administration has some advantages as far as the transfection efficacy to DCs by Man-lipoplex is concerned; this is because of (i) high accessibility to APCs in the peritoneal cavity and lymph nodes, (ii) long retention of the lipoplex, (iii) the presence of few biocomponents that reduce transfection activity, and (iv) the high capacity of the lipoplex solution. Taking these factors into consideration, i.p. administrated Man-lipoplex would enhance gene expression in APCs resulting in efficient DNA vaccine therapy. However, few reports are available on the effect of i.p. administered Man-lipoplex on DNA vaccine therapy.

The objective of this paper was to clarify the DNA vaccine potency after i.p. administration of Man-lipoplex. In the present study, ovalbumin (OVA)-encoding pDNA (pCMV-OVA) was selected as a model DNA vaccine. Using *in vitro* and *in vivo* experiments, the transfection efficacy to APCs was evaluated by measuring the OVA mRNA using quantitative reverse-transcription polymerase chain reaction (RT-PCR). After immunizing with Man-lipoplex, OVA-specific CTL responses and its antitumor effects against inoculated E.G7-OVA cells (OVA expressing cells), and its parental cell line, EL4 cells (OVA non-expressing cells), were also evaluated. The results obtained were compared with those of conventional lipoplex and naked pCMV-OVA.

Materials and methods

Materials

Cholesteryl chloroformate, HEPES, concanavalin A, G418, and immunogloblin G were obtained from Sigma Chemicals Inc. (St. Louis, MO, USA). *N*-[1-(2,3-Dioleyloxy)propyl]-*N*,*N*,*N*-trimethylammonium chloride (DOTMA) and *N*-(4-aminobutyl)carbamic acid *tert*-butyl ester were obtained from Tokyo Chemical Industry Co. (Tokyo, Japan). Dioleoylphosphatidylethanolamine (DOPE) was purchased from Avanti Polar Lipids, Inc. (Alabaster, AL, USA). pVAX I, fetal bovine serum (FBS), and Opti-MEM I® were obtained from Invitrogen Co. (Carlsbad, CA, USA). Anti-CD11c monoclonal antibody (N418)-labeled magnetic beads were purchased from Miltenyi Biotec Inc. (Auburn, CA, USA). Nucleic acid purification kit magextractor®-RNA was purchased from Toyobo Co., Ltd. (Osaka, Japan). The first strand cDNA synthesis kit for RT-PCR, Lightcycler™ faststart DNA master hybridization probes, and a Lightcycler™-Primer/Probes set for mouse β-actin were purchased from Roche Diagnostics Co. (Indianapolis, IN, USA). Primers/probes for OVA were purchased from Nihon Gene Research Labs Inc. (Miyagi, Japan). All other chemicals were of the highest purity available.

Animals

Female ICR mice (4–5 weeks old) and C57BL/6 mice (6–8 weeks old) were purchased from the Shizuoka Agricultural Cooperative Association for Laboratory Animals (Shizuoka, Japan). All animal experiments were carried out in accordance with the Principles of Laboratory Animal Care as adopted and promulgated by the US National Institutes of Health and the guideline for animal experiments of Kyoto University.

Cell line

DC2.4 cells, a cell line of murine dendritic cells (DCs, haplotype H-2b) [25], were kindly provided by Dr. K. L. Rock (University of Massachusetts Medical School, Worcester, MA, USA). The expression of mannose receptors in this cell line has been confirmed elsewhere [26]. Therefore, DC2.4 cells are a suitable model of DCs.